JOURNAL OF GEOPHYSICAL RESEARCH, VOL. 108, NO. A6, 1263, doi:10.1029/2002JA009511, 2003

Identification of the magnetic cloud boundary layers

Fengsi Wei, Rui Liu, Quanlin Fan, and Xueshang Feng

SIGMA Weather Group, Laboratory for Space Weather, Center for Space Science and Applied Research, Chinese Academy of Sciences, Beijing, China

Received 30 May 2002; revised 24 January 2003; accepted 9 April 2003; published 27 June 2003.

[1] Based on a statistical analysis of the boundary physical states of 80 magnetic clouds reported in the literature from the years 1969 to 2001, we suggest a new identification of the magnetic cloud boundary by describing it as front and tail boundary layers (BLs) formed through the interaction between the magnetic cloud and the ambient medium. In our identification the outer boundary of the layer often displays the properties of magnetic reconnection, which could be characterized by a ''three-high state'' (relatively high proton temperature, high proton density, and high plasma beta) and the corresponding magnetic signatures (the intensity drop and the abrupt azimuthal changes, $\Delta\phi \sim 180°$, and latitudinal changes, $\Delta\theta \sim 90°$, in the magnetic field). The inner boundary of the layer exhibits a ''three-low state'' (relatively low proton temperature, low proton density, and low plasma β) and separates the magnetic cloud body, which has not basically been affected by the interactions, from the boundary layers. The front boundary layer could be associated with the outer loops of CMEs and its average time scale is 1.7 hours; the tail boundary layer seems not be a filament and its average time scale is 3.1 hours. The distribution function of magnetic fluctuations in the boundary layer is significantly different from those in the ambient solar wind and the cloud body itself. The preliminary numerical simulation in principle confirms this new identification and could qualitatively explain most of the observations of the cloud boundary. This work could help partly overcome some inconsistencies in identifying the boundaries of magnetic clouds. *INDEX TERMS:* 2111 Interplanetary Physics: Ejecta, driver gases, and magnetic clouds; 2134 Interplanetary Physics: Interplanetary magnetic fields; 7835 Space Plasma Physics: Magnetic reconnection; 2164 Interplanetary Physics: Solar wind plasma; *KEYWORDS:* magnetic clouds, magnetic reconnection, boundary layer

Citation: Wei, F., R. Liu, Q. Fan, and X. Feng, Identification of the magnetic cloud boundary layers, *J. Geophys. Res.*, *108*(A6), 1263, doi:10.1029/2002JA009511, 2003.

1. Introduction

[2] The concept of magnetic clouds is the combination of the frozen-in magnetic field and of the plasma clouds that had been proposed since the 1950s and even before [*Chapman and Ferraro*, 1929; *Morrison*, 1954; *Cocconi et al.*, 1958; *Gold*, 1962; *Burlaga et al.*, 1981]. The term of magnetic clouds was first introduced by Burlaga et al. in 1981. The necessary conditions to identify a magnetic cloud [*Klein and Burlaga*, 1982; *Burlaga*, 1991, 1995; *Osherovich and Burlaga*, 1997] are (1) enhanced magnetic field strength, (2) a smooth rotation of the magnetic field direction through a large angle during the interval of the order of one day, and (3) low proton temperature and low plasma β. As an important and distinct subset of interplanetary large-scale transient structures, magnetic clouds have been intensively investigated, but many questions remain open. How to identify the magnetic cloud boundary is a question that has been highlighted in the literature [*Burlaga*, 1991, 1995; *Farrugia et al.*, 1997] and is also the main topic we will discuss in this paper. In addition, the research of the cloud boundaries is associated with many important problems, such as its relation with CMEs, the interaction between the clouds and the solar wind flows, the cloud-geomagnetosphere coupling.

[3] The identification of the boundaries of magnetic clouds is a difficult problem. Many signatures have been used to identify the boundaries of magnetic clouds [e.g., *Burlaga et al.*, 1980; *Marsden et al.*, 1987; *Gosling et al.*, 1987; *Osherovich et al.*, 1993; *Farrugia et al.*, 1994; *Fainberg et al.*, 1995; *Tsurutani et al.*, 1988; *Tsurutani and Gonzalez*, 1997; *Burlaga*, 1995; *Lepping et al.*, 1997], such as temperature decrease, density decrease, directional discontinuity, magnetic hole, bidirectional streaming of suprathermal electrons or low energy protons, deviation from the Maxwell distribution of the electrons, and abrupt decrease in the intensity of low energy protons and plasma β. However, as *Burlaga* [1995] indicated, there is no consistency among the various approaches to identify magnetic cloud boundaries. For example, we can see in a case reported by *Burlaga et al.* [1980], the magnetic hole preceded the drop in temperature by about 1 hour and no consistency existed between low temperature and low

0148-0227/03/2002JA009511$09.00

density. *Farrugia et al.* [1997] also pointed out that the determination of cloud boundaries and their nature is an urgent research problem.

[4] Magnetic clouds are part of the interplanetary manifestations of Coronal Mass Ejections (CMEs). The relationship between magnetic clouds and structures of CMEs is an interesting topic. It could bring some useful information for further understanding the evolution of CMEs through the corona and interplanetary space. *Gosling* [1997] stated that many CMEs begin as a slow swelling of a coronal streamer on a time scale of several days [e.g., *Hundhansen*, 1997]. These CMEs often appear to have a three-part structure consisting of an outer loop, an inner cavity relatively devoid of material, and an embedded prominence, mirroring the structure of their place of origin lower in the solar atmosphere [*Hundhansen*, 1998]. Till now, each of the three main features of CMEs observed close to the Sun has not been identified at 1 AU. *Tsurutani and Gonzalez* [1997] interpreted the magnetic cloud as being the dark region, since magnetic clouds are characterized by low ion temperatures [*Farrugia et al.*, 1997]. However, what are the interplanetary manifestations of these loops and filaments? *Tsurutani et al.* [1988] analyzed a magnetic cloud observed during 28–29 September 1978 reported by *Galvin et al.* [1987] and suggested that an anomalous region from 0630–0830 UT exists just ahead of the magnetic cloud. This interval is characterized by higher density and temperature plasma, enhanced H^{++}/H^{+} values, and the region is also bounded by magnetic field discontinuities at ~0630 and ~0830 UT. It is speculated that this plasma is the remnants of the bright loops of the CME. They reported that such structure upstream of the magnetic clouds is present 20–40% of the time at 1 AU. *Crooker et al.* [1998] analyzed 14 magnetic clouds near sector boundaries in the period from August 1978 to February 1982 and identified three patterns: (1) half of the clouds occurred at sector boundaries, (2) nearly the same half occurred with longer counter streaming electron events, in contrast to equal or shorter events in clouds away from sector boundary, and (3) most of these longer events concurred with an arch-shaped excursion in magnetic latitude. They suggested that previously documented clouds, identified by magnetic signatures, are only parts of larger transient structures that are best observed in their entirety at sector boundaries, and that the opportunity to sample the larger structures is highest at sector boundaries. The results are consistent with the view that the streamer belt serves as a passageway for most CMEs. *Larson et al.* [1997] reported that five solar impulsive ~1–102 *kev* election events were detected while the Wind spacecraft was inside the magnetic cloud observed upstream of the Earth on 18–20 October 1995. They interpreted these as evidence for patchy disconnection, by magnetic reconnection with adjacent field lines, of one end or both ends of the cloud magnetic field lines from the Sun. They believe the disconnections probably occurred after the ejection of the cloud from the Sun ~4 days earlier. *Collier et al.* [2001] presented the observed particle and field signature of the cloud. They explained that an internal shock wave is evidence for the magnetic reconnection occurring near the root point of the cloud and indicated some ambiguity about the location of the back of the cloud. *Tsurutani et al.* [1998] studied the interplanetary high-speed stream and the resultant first substorm (0332–0334UT) on 10 January 1997 and indicated that a 47 min interval (0219–0302 UT) of relatively intense southward interplanetary magnetic field (IMF) ($B_s = 4 - 8nT$) bounded by two tangential discontinuities (TDs) is identified between the interplanetary shock and the magnetic cloud. They speculated that this IMF B_z structure may be an outer loop. Another similar loop is identified just adjacent to the cloud (0440 ~ 0500 UT). They believed that two such loops have been identified in the Wind magnetic field data. We suggest that the boundary layers proposed in this paper, especially the front boundary layers of magnetic clouds, could be the remnants of these loops.

[5] The interaction between the magnetic cloud and the background solar wind is a complex problem which makes the identification of the cloud boundary difficult. *Lepping et al.* [1997] suggested that the magnetic cloud, whose beginning was at 1858 UT on day 291, 1995, was being overtaken by a corotating stream. The stream apparently compressed the plasma and field at the rear of the magnetic cloud. A stream interface was seen at 2254 UT on day 292. It results in some difficulty in determining the tail boundary of the cloud on 18 October 1995. *Janoo et al.* [1998] analyzed field and flow perturbations in the magnetic cloud and found that there are a number of magnetic field directional discontinuities (DDs) and explained that the changes in proton temperature across these DDs suggest a more elaborate structure, for example, a reconnection layer. They suggested that the field directional discontinuities D1, namely the front boundary of the cloud, is included in the reconnection layer. *Lepping et al.* [1997] analyzed the cloud's interplanetary properties as triggers for geomagnetic activity and indicated that the front boundary of the magnetic cloud at 1858 UT on day 291 was a magnetic hole, i.e., a small-scale magnetic structure in which the field strength is low, with beginning and ending times at 1856: 19.5 and 1900: 16.5 UT, across which the total pressure was approximately constant and the magnetic field direction rotated through 176° in a plane. *Burlaga* [1995] indicated that this is not an unusual feature at the front boundary of a magnetic cloud.

[6] The cloud-geomagnetosphere coupling is a very important aspect in space weather study in which space weather effects of magnetic clouds on geomagnetic field activities and galactic cosmic rays are intensively investigated [e.g., *Farrugia et al.*, 1996, 1997; *Gonzalez and Tsurutani*, 1987; *Zhang et al.*, 1988; *Tsurutani et al.*, 1992]. The nature of a number of discontinuities in the sheath driven by clouds is closely associated with the geomagnetic activity. *Farrugia et al.* [1994] gave a possible magnetic barrier ahead of the 29–30 September 1978 magnetic cloud. Farrugia et al. [2001] examined a 3-hour-long interval on 24 December 1996 observed at Wind, a rotational discontinuity and a slow shock. They reported that the Wind spacecraft at 1 AU observes two sets of perturbations and interpreted that the second is a reconnection layer at ~0126 UT, 24 December 1996, taking place between field lines of a CME of which the magnetic cloud formed a part. *Tsurutani et al.* [1998] speculated that an outer loop in the interval (0219–0302 UT) leads to the auroral hotspot, the theta aurora, and the horseshoe aurora, of the CME coming from the Sun. *Farrugia et al.* [1998]

analyzed unusual features of the 10 January 1997 magnetic cloud and found that there is a thin plasma depletion layer (PDL) (0437–0458 UT, 10 January 1997) preceding the cloud. PDLs, strongly southward field in PDL/cloud, can be important at the outer edge where the magnetic field rotates southwards with high temperature and low pressure because they may elicit major effects in the Earth's magnetosphere-ionosphere system. *Tsurutani and Gonzalez* [1997] indicated that the two interplanetary regions are important for intense southward IMFs: the sheath region just behind the forward shock and the ejecta material itself. If the fields are southward in both the sheath and solar ejecta, two-step main phase storms can result. The storm main phase occurs in near coincidence with the sharp southward turning of the IMF at the magnetic cloud boundary. *Tsurutani et al.* [1988] further studied the origins of the interplanetary southward B_z which cause the 10 major magnetic storms (Dst < -100 nT) detected during the 500 days from 16 August 1978 to 28 December 1979 and indicate the equal importance of both sheath fields or draped fields and driver gas fields for the generation of major geomagnetic storms. Because of the importance of the sheath fields the intensity and duration of geomagnetic storms cannot be predicted by solar observations of active regions alone.

[7] The purpose of the present work here is to propose a new identification of the magnetic cloud boundary based on the analysis of the physical states of cloud boundaries. In section 2, 80 typical magnetic clouds from the year 1969 to 2001, which have been identified in the literature and have few data gaps that may bring up ambiguities, are used in a statistical analysis of the physical states of the magnetic cloud boundaries. On the basis of this analysis, a definition of the magnetic cloud boundary layer and its possible formation mechanism is proposed. To explore the formation mechanism of the cloud boundary layer, a numerical simulation, which corroborates the physical scenario illustrated in section 2, is performed in section 3. Section 4 deals with the magnetic field probability distribution function in the boundary layer, which is distinctly different from those in the ambient medium and inside the cloud.

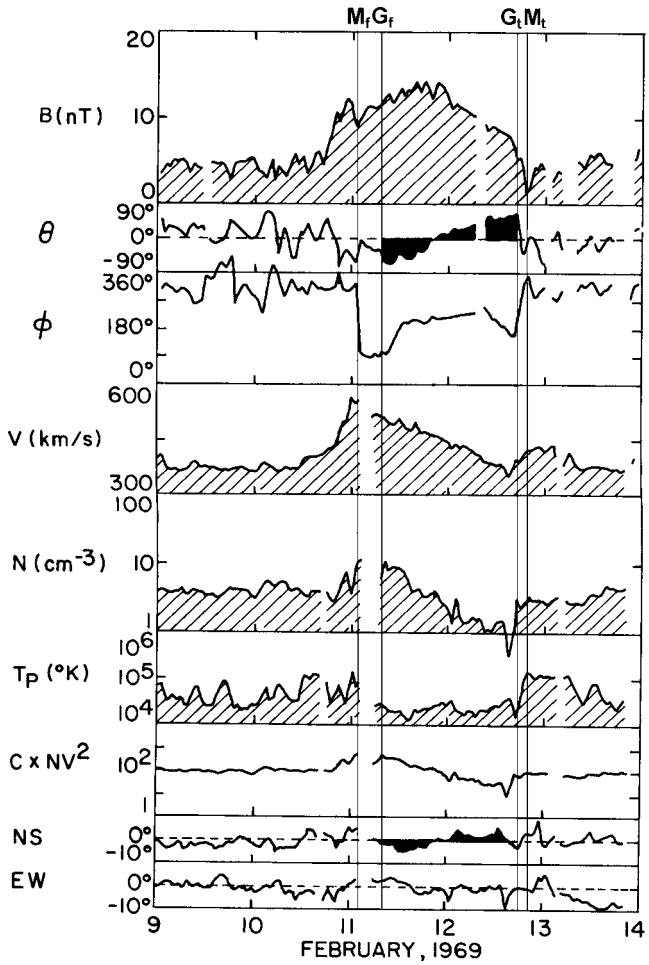

Figure 1. A typical magnetic cloud observed at 11 February 1969 [*Klein and Burlaga*, 1982]. The vertical lines labeled with G_f and G_t indicate the front and tail boundaries determined by *Burlaga et al.* [1981], the vertical lines labeled with M_f and M_t show the boundaries identified by the authors, and the lines labeled with "S" and "C" indicate the shock ahead of the cloud and the center of cloud, respectively.

2. Statistical Study

2.1. Observational Analysis

[8] We tried to find out the basic physical features of the magnetic cloud boundary through the analysis of a great deal of observational data. We collected 80 magnetic cloud events with relatively complete observational data available, which have been either identified in the literature from the year 1969 to 2001 [*Klein and Burlaga*, 1982; *Zhang and Burlaga*, 1988; *Lepping et al.*, 1990, 2001; *Wilson*, 1990; *Bothmer*, 1993] or published on the website of Wind MFI team http://lepmfi.gsfc.nasa.gov/mfi/mag_cloud_pub1.html. Below, we discuss several examples of magnetic clouds to understand the complexity in identifying the boundaries of magnetic clouds.

2.1.1. Case 1

[9] A typical magnetic cloud observed during 11–13 February 1969, first reported by *Klein and Burlaga* [1982], is shown in Figure 1, in which the two vertical lines indicated by letters G_f and G_t, respectively, show the front and tail boundary identified by Klein and Burlaga (hereafter the front and tail boundaries identified by other authors are also labeled with letters G_f and G_t), who mainly took into account the enhancement of the magnetic field strength, B, the smooth rotation of the magnetic latitude angle, θ, and the decrease in the proton temperature, T. Such a determination is of some ambiguity and does not rest on the basis of clear physical concepts, as *Burlaga* [1991, 1995] has admitted. For example, at the G_f boundary, no evident changes in the solar wind parameters were observed, so it is not necessary to choose this position as the cloud boundary. However, just ahead of the G_f boundary, basic features of a magnetic reconnection region could be obviously seen: a depression in the magnetic field strength, abrupt changes in the corresponding magnetic azimuth φ and latitude θ angles, with enhanced proton density, N, and proton temperature, T. Similar changes in the solar wind parameters can be found following the G_t boundary. In this paper the magnetic signatures, including a drop in the field strength and the corresponding abrupt changes in the mag-

netic azimuth and latitude angles, will be used as a new criterion in identifying the cloud boundaries. According to our new criterion, we located the front and tail boundaries of the cloud by two vertical lines labeled with letters M_f and M_t in Figure 1, respectively. An obvious feature of the M boundary (including M_f and M_t) is its close association with plasma parameters with higher density, temperature, and plasma β. In addition, the size of the cloud, bounded by M_f and M_t boundaries, is larger than that of the cloud bounded by G_f and G_t boundaries. A possible reason is that monotonic changes in the magnetic latitude angle, θ, is an important factor in identifying G_f and G_t boundaries, whereas the feature of abrupt changes in the magnetic azimuth angle, ϕ, and the corresponding drop of the field strength are emphasized in our determination of M_f and M_t boundaries. As *Crooker et al.* [1998] suggested, previously documented clouds, identified by magnetic signatures, are only parts of larger transient structures. They indicated that the former authors focused on the initial rotation in θ, whereas the latter focused on the rotation in ϕ. As *Lepping et al.* [1990] stated, locating cloud boundaries is a matter of subjective judgment. Moreover, since these authors constrained their choices to monotonic changes in the latitudal angle, they were also aware that their choices represent lower limits on cloud sizes [e.g., *Zhang et al.*, 1988].

2.1.2. Case 2

[10] A magnetic cloud preceded by a shock, with the magnetic field magnitude greater than 20 nT and its time scale about one day, is shown in Figure 2. It was observed by the Wind spacecraft at 1 AU on 19 October 1998. In this case there are no significant structures inside the magnetic cloud, except a dip in the magnetic field strength at the hour of 47. We can see from Figure 2 that both the M_f and the M_t boundaries are associated with depression in the magnetic filed strength, abrupt directional changes in the corresponding azimuth and latitude angles, and the enhanced proton temperature, proton density, and plasma β relatively to the cloud's proper values. However, the G_f and G_t boundaries are associated with a higher magnetic field magnitude, an initial smooth rotation in the latitude angle, and a relatively low proton temperature, a low proton density, and a low plasma β. The time intervals are about 3 hours for the M_f and G_f boundaries and about 1 hour for the M_t and G_t boundaries. An interplanetary sheath beginning at $\sim$1940 UT on 18 October 1998 can also be seen in Figure 2, which is a shock compression region driven by the cloud. Its main features include higher magnetic field, temperature, and density structure, a shock discontinuity ahead of the sheath, larger, frequent fluctuations in the field directions. These features are distinctly different from those of M_f and M_t boundaries, marked by an abrupt drop in the magnetic field strength and abrupt directional changes in ϕ and θ angles in the meantime. According to the criterion used by *Tsusutani et al.* [1998] in identifying the bright loop ahead of the magnetic cloud on 10 January 1997, we speculate that the region bounded by two magnetic directional discontinuities (at 2600 UT and $\sim$2800 UT) could be a so-called bright loop structure adjacent the cloud, which differs obviously from that of the sheath. About 20 similar bright loops may exist at front boundary layers in the 80 magnetic clouds investigated in the paper (see below). Though to identify them carefully is beyond the scope of this paper, it deserves noticing that these loops are not simply convected outward but are undergoing certain complicated interactions.

2.1.3. Case 3

[11] A magnetic cloud with a relatively strong magnetic field, preceded by a shock and containing an internal shock wave, was observed by WIND spacecraft during 18–19 October 1995 (Figure 3). In this case, the cloud's total pressure, the sum of the proton thermal pressure, and the magnetic pressure is ten times higher than the background solar wind, which drove a fast MHD shock ahead of the cloud. A notable feature is that the M_f boundary with lower field strength B_t, higher proton temperature T, proton density N, and plasma β is nearly coincident with the G_f boundary with higher B_t and lower T, N, and β. The time interval between them is about 5$\sim$6 min, as a magnetic hole shown by *Lepping et al.* [1997] in the form of 3 s averages of the magnetic field. The G_t boundary is associated with relatively low proton temperature and proton density but no change in plasma β is seen, while the M_t boundary is associated with higher proton temperature, proton density, and plasma β, namely the so-called "hhh" state. This magnetic cloud is a very typical event extensively investigated by many authors [e.g., *Collier et al.*, 2001; *Janoo et al.*, 1998; *Larson et al.*, 1997; *Lepping et al.*, 1997; *Chao et al.*, 1999]. *Lepping et al.* [1997] indicated that the front boundary of the cloud at 1858 UT on the day of 291 (DOY) was associated with a magnetic hole with beginning and ending times of 1856:19.5 and 1900:16.5 UT, where the magnetic field direction rotated through about 176°. The magnetic hole is consistent with the M_f boundary identified by us. They also suggested that a corotating stream was overtaking the magnetic cloud and a stream interface was seen at 2254 UT on the day of 292. This corotating stream may cause the ambiguity in identifying the G_t boundary. *Collier et al.* [2001] explained that an internal shock wave beginning at $\sim$1800 UT on the day of 292 is an evidence for the magnetic reconnection occurring near the foot point of the cloud and indicated some ambiguity about the location of the tail boundary. We think that the internal shock-like structure, at least, has not been affected by the corotating stream because the overtaking effects have not been reflected in the plasma temperature, velocity, and plasma β. *Janoo et al.* [1998] found that there are a number of magnetic field directional discontinuities (DDs) during 18–19 October 1995 and suggested that the discontinuity D1 at $\sim$1900 UT on the day of 291 (i.e., G_f boundary) is a reconnection layer. It should be noticed that a region with a higher density, temperature, a moderate field strength higher than the sheath field and lower than the cloud field, and bounded by two magnetic directional discontinuities beginning at $\sim$1600 UT and ending at $\sim$1900 UT, according to the criterion proposed by *Tsurutani et al.* [1998], would be a so-called bright loop of a CME. The region owns the structure obviously different from that of the sheath, which is similar to the structure bounded by the M_f and G_f boundaries in Figure 2. Of course, this is only a speculation.

2.1.4. Case 4

[12] A pressure-balanced weak magnetic cloud overtaken by a shock observed by Wind spacecraft on 3–4 October 2000 is shown in Figure 4. Its temperature and plasma β parameter are almost constant except for some fluctuations

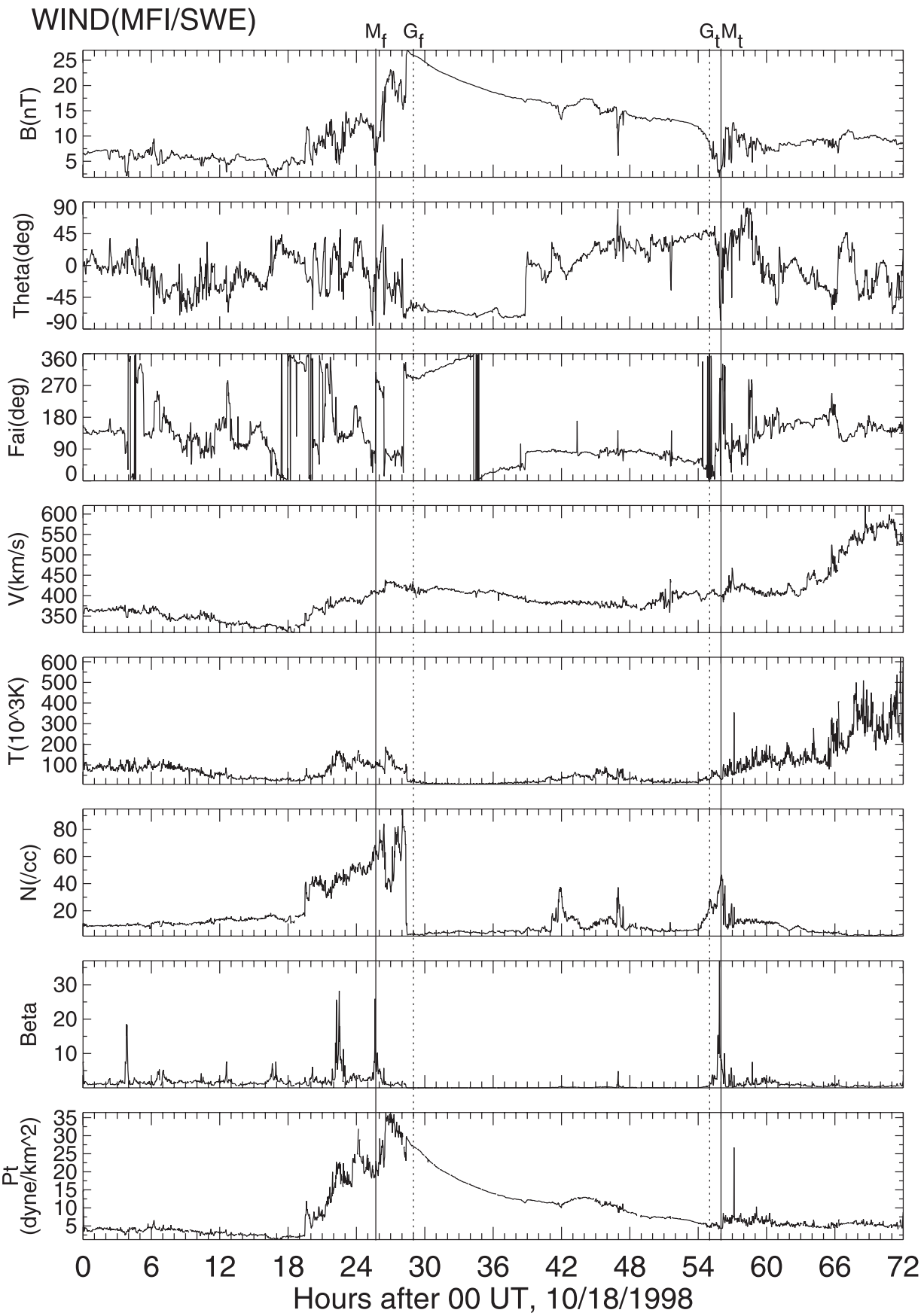

Figure 2. A magnetic cloud preceded by a shock was observed by Wind during 19–20 October 1998. The panels show from top to bottom the magnetic field magnitude, its latitude and azimuthal angels, θ and ϕ, in GSE coordinates, the proton temperature, density and velocity, plasma β, and total pressure.

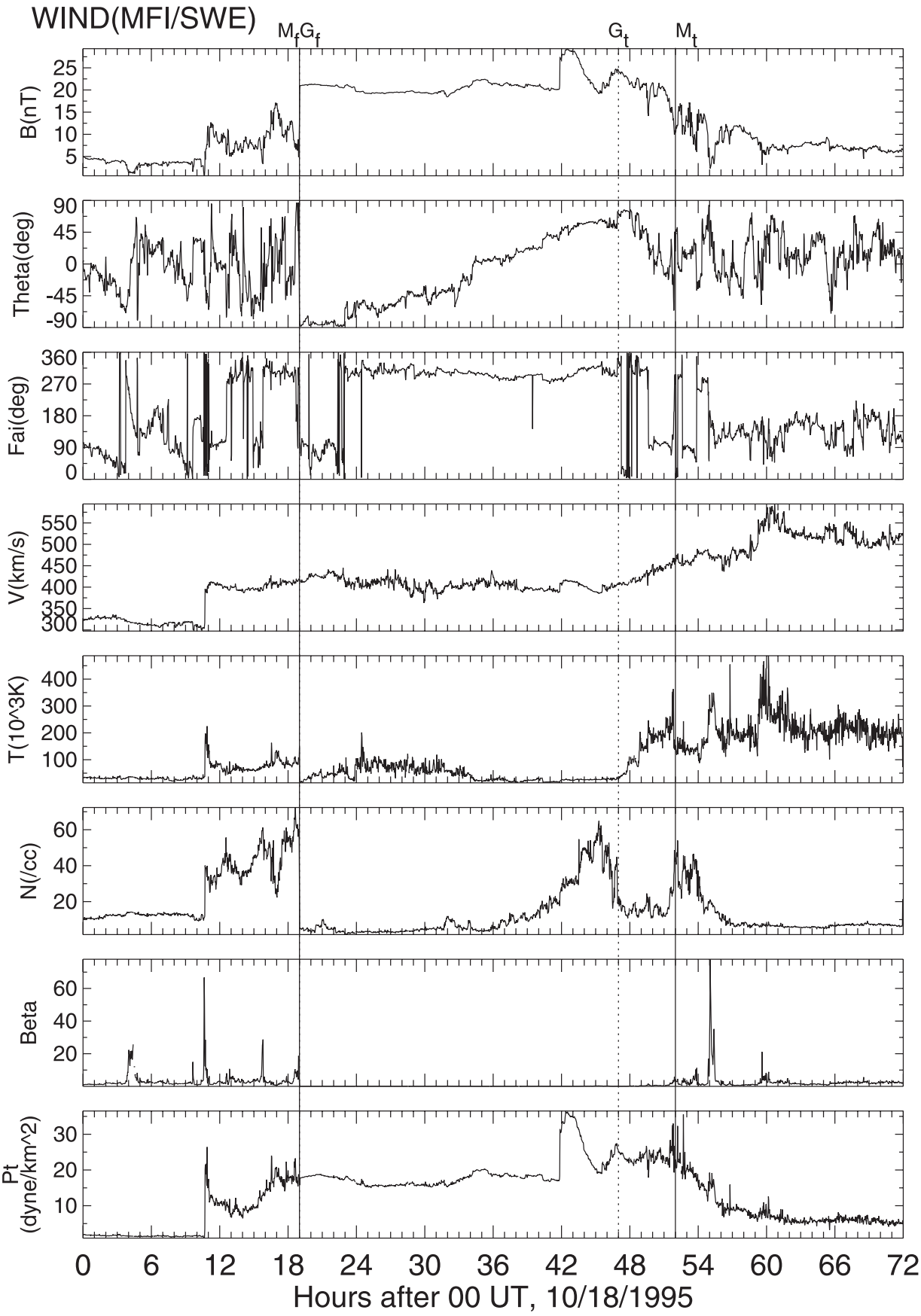

Figure 3. A magnetic cloud observed by Wind during 18–20 October 1995. This cloud with relatively strong magnetic field is preceded by a shock and contains an internal shock-like structure at about 2000 UT, 19 October 1995.

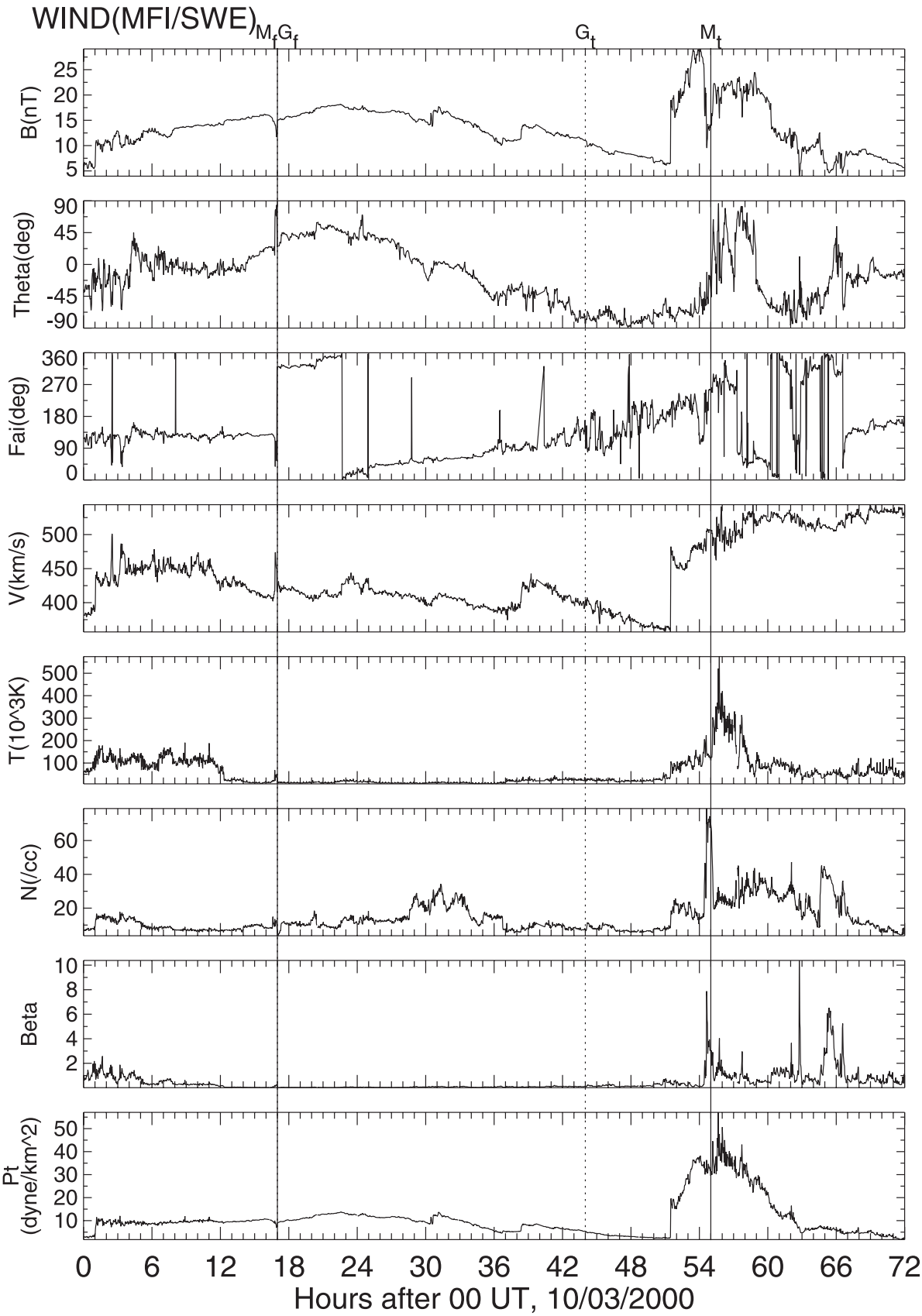

Figure 4. A magnetic cloud observed by Wind during 3–5 October 1996. This cloud is almost pressure-balanced with the background solar wind at its front part and is overtaken by a shock. The M_f and G_f boundaries are almost coincident with each other, while the G_t and M_t boundaries are far from each other.

in the density. In this case the M_f and G_f boundaries are nearly coincident with each other, but a larger time interval of about 11 hours appears between the M_t and G_t boundaries, in fact the region beginning at ~2000 UT on 3 October and ending at ~0330 UT on 4 October, still tends to preserve the cloud's characteristics. From Figure 4 we can see that the magnetic annihilation amplitude is so small that there are only very slight increases in the proton temperature, proton density, and plasma β at the M_f boundary, though the field direction rotated about 180°. As there are no obvious changes in the proton temperature and density at the G_t boundary, it is questionable if this G_t boundary could be the real tail boundary. The tail of the cloud shows certain complete ''sheath'' structures with lasting higher field strength, temperature, density, and velocity, since the magnetic cloud was overtaken by the shock wave. However, a prominent depression in the magnetic field strength and corresponding increases in the solar wind parameters are still observed at the M-tail boundary, although this structure is swept over by the shock.

2.1.5. Case 5

[13] A magnetic cloud with a relatively weak magnetic field strength of about 12 nT observed by Wind spacecraft during 24–25 December 1996, without any significant structures ahead of and behind the cloud, is shown in Figure 5. The time interval between the boundaries is about 1 hour, either for the M_f and G_f or M_t and G_t boundaries. In this case the magnetic signatures are very clear both in the drop of the field strength and the abrupt changes of field directions. Both the M_f and M_t boundaries are associated with the ''hhh'' state, namely relatively high proton temperature, proton density, and plasma β, although these enhancements in the tail boundary are small. However, the G_f and G_t are associated with the ''LLL'' state, namely, relative low proton temperature, proton density, and plasma β.

2.1.6. Case 6

[14] A magnetic cloud with a relatively small time scale of about 4 hours, observed by the Helios 1 spacecraft at 0.75 AU on 25 June 1979, is shown in Figure 6. Although the front and tail parts of the cloud present complex solar wind structures, we can still see that the M_f and M_t boundaries are associated with a drop in the field strength, abrupt changes in the azimuth and latitude angles, and a relatively high proton temperature, proton density, and plasma β, i.e., ''three high'' states. However, the G_f and G_t boundaries correspond to relatively low proton temperature, proton density, and plasma β. Why does the magnetic cloud have such a small temporal scale at 0.75 AU? Does this cloud originate from a small CME? Is it possible that its magnetic field have been rapidly peeled off through the magnetic reconnection processes when the cloud propagates outwards away from the Sun? Further analysis of its solar origin and interplanetary evolution may broaden our knowledge of cloud dynamics.

2.1.7. Case 7

[15] A magnetic cloud with an upstream shock and a steam-stream interaction region behind, observed at 0.86 AU by Helios 1 on 8 June 1977, is shown in Figure 7. The M_f boundary can be identified without ambiguity by using the new criterion mentioned in Case 1, while the tail part of the cloud, overtaken by the stream interface, seems to ''merge'' into the background solar wind, which makes the determination of the M_t boundary very difficult. We can see that a shocked sheath ahead of the cloud is a compressed plasma region, which can be distinguished from the M_f boundary marked by a field dip, higher temperature, density, and plasma β and followed by gradual decreases in plasma parameters for about 2 hours until reaching the cloud's proper value. It should be noticed that an interesting structure, with higher density, lower temperature, and higher field strength and bounded by two magnetic directional discontinuities, beginning at ~1230 UT and ending at ~1600 UT on 8 June, is embedded in the sheath. We speculate that this structure is also an outer loop of the CME associated with the cloud, as shown in Figure 2.

[16] From the examples mentioned above, we can see that the identification of the magnetic cloud boundary is a difficult task and still partly subjective because it is associated with many complex problems, such as CME structures, their evolution, and interaction with the background solar wind, especially in the determination of tail boundaries. The G_f and G_t boundaries identified in the literature often correspond to various physical states, while M_f and M_t boundaries, identified by the magnetic signatures characterized by the magnetic intensity depression and abrupt changes in the corresponding latitude and azimuthal angles, are almost always associated with the ''hhh'' physical state. Thus the following questions should be considered: Does the M boundary exist only in cases mentioned above or is it more general? What are the physical characteristics of the M boundary? What is its connection with G boundary? Is it possible to define the cloud boundary based on a clear physical picture? Only when we look at a great number of cases and look for subtle but significant trends do we see the generalizations. In what follows, we determine the M boundaries (including M_f and M_t) of 80 magnetic clouds based on the new criterion and label the boundaries identified by other authors, i.e., the G boundaries (including G_f and G_t) given in Table 1. The physical states of the two kinds of boundaries are depicted by the three general solar wind parameters: proton temperature T, proton density N, and plasma β. The states of each physical parameter are respectively recorded by letters h, m, L, and n, indicating that their readings are relatively high (h), middle (m), low (L), and no change (n) to the adjacent background value of the boundary, respectively. In consequence, we get 64 combinatory states of three parameters T, N and β. The three parameters line in the order of T, N, and β, for example, if T is in ''h'' state and the other two parameters, N and β, are in any of the four states, ''h,'' ''m,'' ''L,'' and ''n,'' we get 16 combinatory physical states: hhh, hhm, hhL, hhn, hmh, hmm, hmL, hmn, hLh, hLm, hLL, hLn, hnh, hnm, hnL, and hnn (note that the first letter represents the temperature). By analogy, the rest of the combinatory states

Figure 5. (opposite) A magnetic cloud observed by Wind during 24–25 December 2000. This cloud with relatively weak field strength is bounded by two magnetic-hole-like structures, where its M_f and M_t boundaries are identified by the authors.

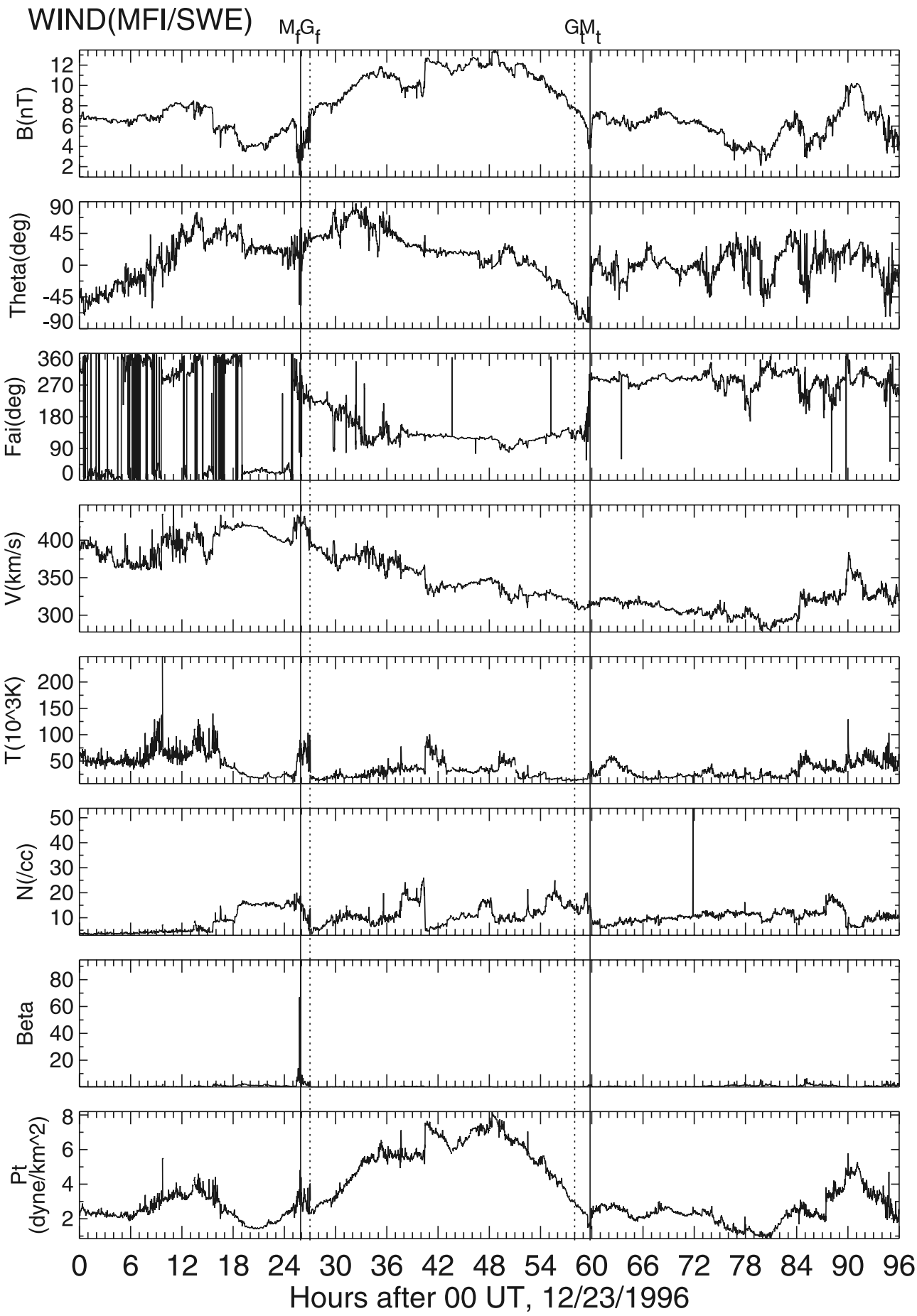
WIND(MFI/SWE)
M_fG_f
G_tM_t
B(nT)
Theta(deg)
Fai(deg)
V(km/s)
T(10^3K)
N(/cc)
Beta
Pt (dyne/km^2)
0 6 12 18 24 30 36 42 48 54 60 66 72 78 84 90 96
Hours after 00 UT, 12/23/1996

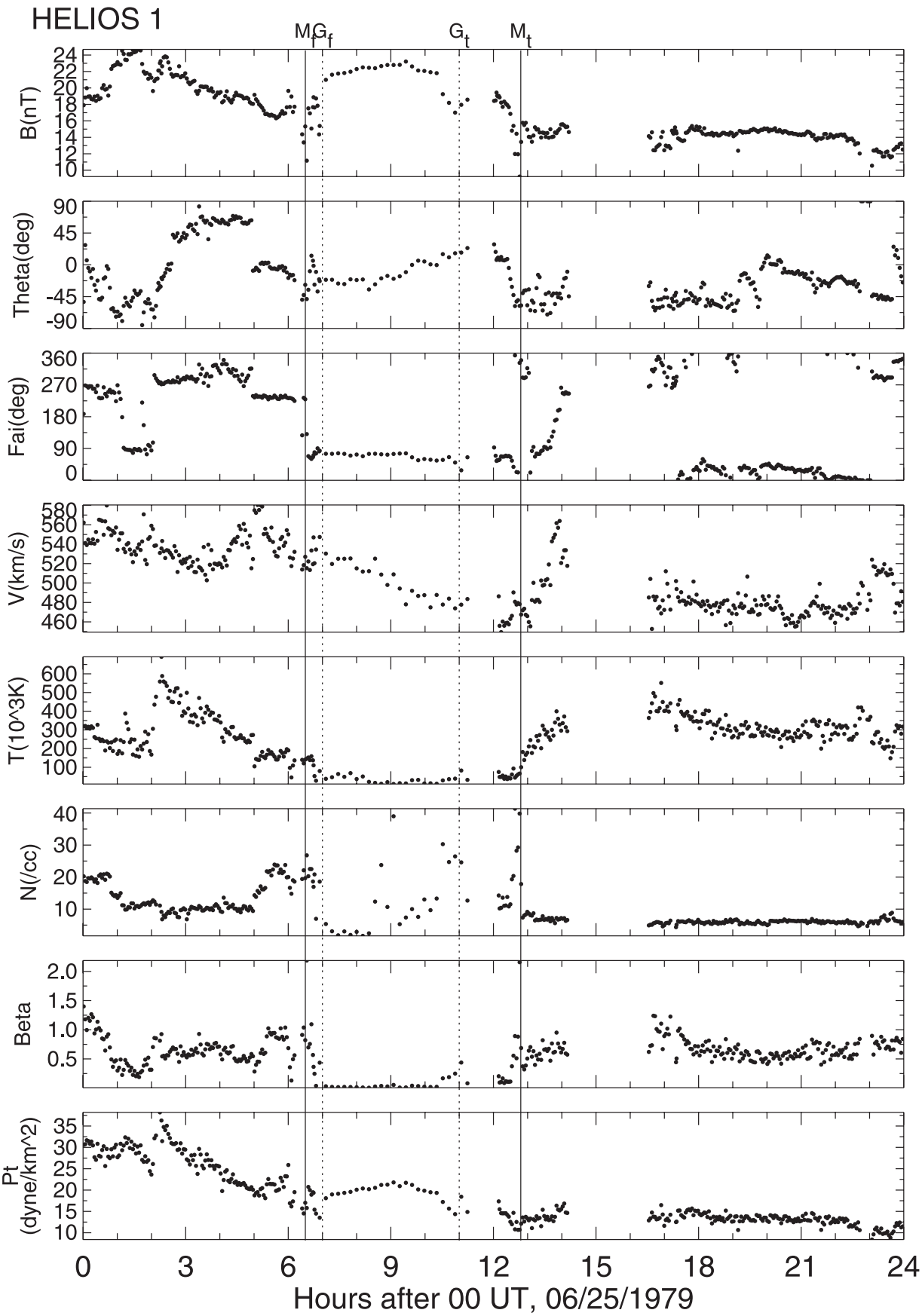

Figure 6. A magnetic cloud with relatively small scale observed by Helios 1 on 25 June 1979. Like Figure 5, this cloud is also bounded by two magnetic-hole-like structures.

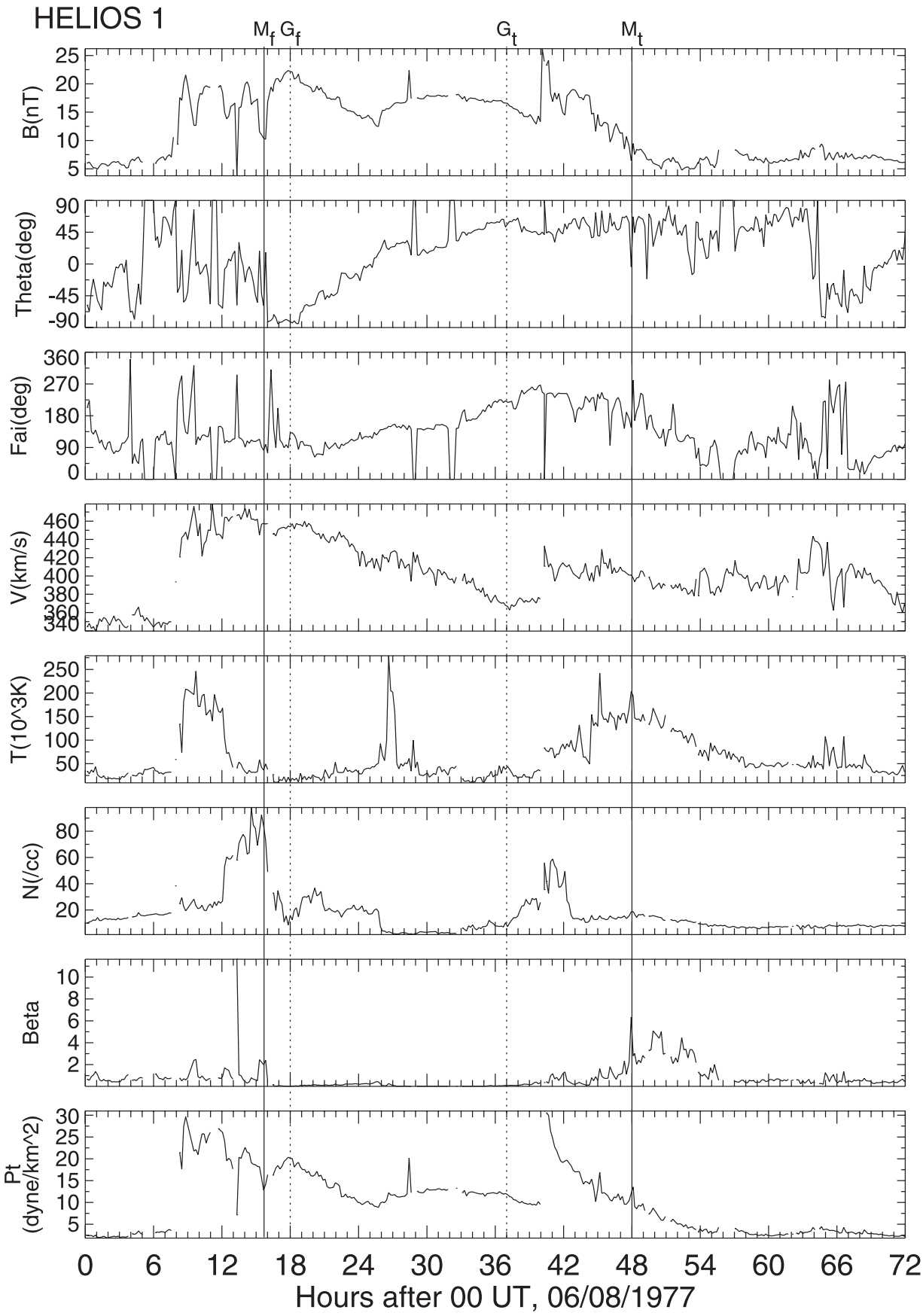

Figure 7. A magnetic cloud observed by Helios 1 during 8–9 June 1977. This cloud is preceded by a shock and overtaken by a stream-stream interaction region.

Table 1. List of Magnetic Clouds Investigated in This Paper[a]

	Start	End	Physical States, TNβ				Δt, hr			
	yy/ddd/hh	ddd/hh	G_f	G_t	M_f	M_t	$M_f - G_f$	$M_t - G_t$	R, AU	Data Source
1	69/042/09	043/17	Lhm	Lhm	hhh	hhh	−7.0	+2.0	1.0	IMP8
2	73/091/22	092/22	Lhm	LmL	hhm	hnh	−2.0	+3.0	1.0	IMP8
3	75/007/00	007/10	mmm	hLm	hhh	hhh	−2.0	+1.0	0.92	Helios1
4	75/063/16	064/05	mLL	mhm	hmh	hhh	−1.0	0.0	0.4	Helios1
5	75/092/06	092/15	nmn	LmL	nhh	hnh	−2.6	1.5*	0.48	Helios1
6	75/145/16	147/02	mhm	mnm	mhm	hhh	0.0	+2.0	1.0	IMP8
7	75/213/04	214/03	mmL	mLL	mhh	hhh	−3.0	+2.0	1.0	IMP8
8	75/313/02	313/18	nhm	hLh	nhm	hnh	0.0	+ 3.7	0.81	Helios1
9	75/321/02	322/05	hhh	mmm	hhh	hhh	−1.0	+3.0	1.0	IMP8
10	76/072/16	073/22	Lhm	nhh	Lhm	nhh	0.0	0.0	0.5	Helios1
11	76/073/10	074/08	mnm	mhL	mnm	LLm	0.0	+3.0	0.7	Helios2
12	76/090/09	090/21	mhh	mhn	mhh	mnn	+ 0.5	+4.0	0.46	Helios2
13	76/187/03	187/21	LLL	nnn	hhh	hhh	−1.5	+2.0	0.98	Helios1
14	77/029/10	030/10	hhh	nnn	hhh	nhh	0.0	+2.0	0.95	Helios1
15	77/063/12	063/17	LhL	hnh	hhh	hnh	−1.0	0.0	0.74	Helios1
16	77/076/05	076/20	LLL	mnm	Lhh	hnh*	−1.8	+5.0*	0.71	Helios2
17	77/159/18	160/13	nLn	nLn	hhh	hnh	−2.0	+11.0	0.86	Helios1
18	77/240/14	241/10	nhn	mLL	Lhh	hhh	−1.0	+2.0	0.8	Helios1
19	77/335/14	336/00	LLL	nhn	mhh	hhh	0.7	16.0*	0.75	Helios1
20	78/004/08	005/10	LLL	hnn	hhh	hhh	−0.5	+9.0	0.94	Helios2
21	78/006/13	008/14	mmL	mmm	hhh	hhh	−2.5	+2.5	2.0	Voyager1
22	78/037/16	038/16	LLL	nmn	hhh	nhh*	−0.5	+6.0*	0.97	Helios2
23	78/046/14	047/20	LLL	Lnn	hhh	hmh	−1.7	+2.0	0.94	Helios1
24	78/061/01	62/1.0	LLL	nmn	hhh	hnh*	−3.0	+17.0*	0.9	Helios1
25	78/239/18	240/18	LLL	LLL	hhh	hhh	0.5	0.5	1.0	ISEE3,IMP8
26	78/358/15	359/15	LLL	lnn	nhh	hnh	−3.0	+2.0	0.85	Helios2
27	363/09/14	364/14	nLn	LnL	mhh	hhh	−7.0	+2.0	0.8	Helios1
28	79/062/09	062/17	LhL	nmL	hhh	nhh	−2.7	+0.8	0.94	Helios1
29	79/093/02	093/18	hhh	nmn	hhh	hhh*	0.0	+24.0*	0.75	Helios1
30	79/093/21	094/21	mhh	nnn	mhh	hLm	−0.0	+3.0	1.0	IMP/ISEE
31	79/148/23	149/07	LhL	nnn	hhh	hmh	−1.5	+5.5	0.43	Helios1
32	79/176/07	176/11	LLL	nhL	hhh	Lhh	−0.8	+1.6	0.75	Helios1
33	79/261/15	262/18	mLm	hhh	mmh	hhh	−10.0	+1.0	1.0	ISEE3
34	79/286/09	286/16	hnn	hnn	hhn	hhh	−1.6	+4.0	0.72	Helios1
35	80/079/18	081/11	LLL	hhh	LLL*	hhh*	0.0	+11.0	1.0	ISEE3,IMP8
36	80/162/17	163/01	mLL	hmL	hhh	hhh	−2.0	+0.8	0.42	Helios1
37	80/172/02	172/20	hmL	Lnn	hhh	hnh	−1.0	+1.5	0.5	Helios1
38	80/354/12	355/14	mmm	mnm	mhm	hhh	−4.0	+1.0	1.0	ISEE3,IMP8
39	81/117/09	118/03	LLL	nnn	hhh	hnh	−0.4	+8.6	0.79	Helios1
40	81/131/15	132/05	hhh	LLL	hhh	hhh	0.0	+1.7	0.65	Helios1
41	81/146/03	147/07	LmL	nnn	hmh	nhh	−1.7	+2.3	0.47	Helios1
42	81/170/03	170/09	hLL	hhh	hhh	hhh	+ 0.8	+0.0	0.33	Helios1
43	95/039/03	039/23	nhh	mhh	nhh	mhh	0.0	+1.0	0.7	Helios2
44	95/063/11	064/05	nhh	hnh	hhh	hnh	0.0	3.5	1.0	Wind
45	95/147/15	149/08	LLL	LLn	hhh	hhh	−1.0	+3.0	1.0	Wind
46	95/234/22	235/20	LLn	hnh	hhh	hnh	−2.0	+5.4	1.0	Wind
47	95/291/19	293/01	hhh	Lnn	hhh	hhh	0.0	+5.0	1.0	Wind
48	96/148/15	150/07	LLL	LLL	hhh	hhh	−1.0	+5.0	1.0	Wind
49	96/183/17	184/10	nhn	mmn	mhh	hmn	−4.0	+7.0	1.0	Wind
50	96/220/13	221/11	nnn	hmm	hhh	mhh	−5.6	−0.5	1.0	Wind
51	96/359/03	360/11	LLL	LLL	hhh	mhh	−1.0	+0.5	1.0	Wind
52	97/010/05	011/03	LLL	hhh	hhh	mhh	−0.5	0.0	1.0	Wind
53	97/111/15	123/08	nLn	mnn	nhh	nhh	−3.0	+5.0	1.0	Wind
54	97/135/09	136/02	hmL	Lnn	hhn	nnh	−4.0	+4.0	1.0	Wind
55	97/159/22	161/02	nmn	nnL	hhn	hhh	−3.0	−1.0	1.0	Wind
56	97/196/06	197/02	nhh	nnn	mhh	hnh	0.0	+10.0	1.0	Wind
57	97/215/14	216/02	LLn	LLn	mhh	hhh	−3.0	+2.0	1.0	Wind
58	97/261/00	263/12	LLn	hnm	mhh	hnh	+ 3.0	+1.0	1.0	Wind
59	97/264/22	265/24	hhh	mnn	hhh	hnh	0.0	+8.0	1.0	Wind
60	97/274/16	275/23	Lhh	nLL	nhm	nhm	−4.0	+1.0	1.0	Wind
61	97/283/23	285/01	LLn	hnn	mhn	hnn	−1.0	+0.0	1.0	Wind
62	97/311/05	312/13	hhh	nnn	hhh	hhh	0.0	+2.0	1.0	Wind
63	97/326/14	327/19	LLL	mnL	hhh	hnh	−1.0	+2.0	1.0	Wind
64	98/007/03	008/10	LLn	nhn	hmh	nmh	−5.0	+6.0	1.0	Wind
65	98/035/04	036/23	mhh	hLn	hhh	nhh	−1.0	+13.0	1.0	Wind
66	98/063/14	065/07	mmn	nhm	mhn	mhh	+ 1.0	+3.0	1.0	Wind
67	98/122/12	123/18	Lmn	hLn	hhh	mhh	−3.0	+1.0	1.0	Wind
68	98/153/10	153/16	LLL	hmn	hhh	hhh	−0.7	+4.0	1.0	Wind
69	98/175/14	176/17	LnL	nhn	hnh	hhh	−4.5	+6.3	1.0	Wind
70	98/232/10	233/20	mLL	LLL	Lhh	Lhh	−3.0	+0.3	1.0	Wind
71	98/292/05	293/07	LLL	LmL	hhh	mhh	−2.5	+3.0	1.0	Wind
72	99/049/14	050/12	nmn	hLh	hhh	LhL?	−2.0	+1.0	1.0	Wind

Table 1. (continued)

	Start	End	Physical States, TNβ				Δ*t*, hr			
	yy/ddd/hh	ddd/hh	G_f	G_t	M_f	M_t	$M_f - G_f$	$M_t - G_t$	R, AU	Data Source
73	99/106/20	107/21	LLL*	hmm	Lmm*	hhh	−1.0	+4.0*	1.0	Wind
74	00/214/00	214/16	LLL	Lnn	nhh	hnn	−4.0	+2.0	1.0	Wind
75	00/225/06	226/05	mmm	LmL	mLm	nhh	−3.3	+1.0*	1.0	Wind
76	00/277/17	278/20	hhn	nnn	hhn	hhh	0.0	+11.0	1.0	Wind
77	00/287/17	288/17	hmm	LLL	Lhh	hhh	−1.0	+2.0	1.0	Wind
78	00/311/23	312/18	LLL	LLL	Lhh	hhh	−0.8	+0.5	1.0	Wind
79	00/210/21	211/11	Lhn	LhL	hhh	hhh	−6.8	−0.3	1.0	Wind
80	01/078/22	081/10	LLL	LmL	hhh	Lmh	−1.0	+1.3	1.0	Wind

[a]The asterisks in the table indicate the existence of an uncertainty because of data gaps or an ambiguity in determining the cloud boundaries. The column labeled R denotes the cloud's distance from the Sun when it was observed.

can be given. Then the various states for all the M_f and G_f boundaries in the front part and M_t and G_t boundaries in the tail part for 80 magnetic clouds can be determined from the observational data and are given in Table 1, where the asterisk indicates that the physical states of cloud boundaries are determined with some uncertainty because of the existence of data gaps and the difficulty in identifying the boundaries.

[17] Here it should be mentioned that about half of the clouds were preceded by shocked sheaths. Among them, eight sheaths were driven by clouds with the speed >550 km/s near the cloud center; 17 sheaths were driven by clouds with the central speed 450 ∼ 550 km/s; 31 sheaths were driven by clouds with the central speed 400 ∼ 450 km/s; and 24 sheaths were driven by clouds with the central speed <400 km/s. The existence of the sheath seems to have little effect in the identification of the cloud boundaries.

2.2. Statistical Results

[18] The distribution of frequency number of the 64 combinatory states is shown in Figure 8, in which 64

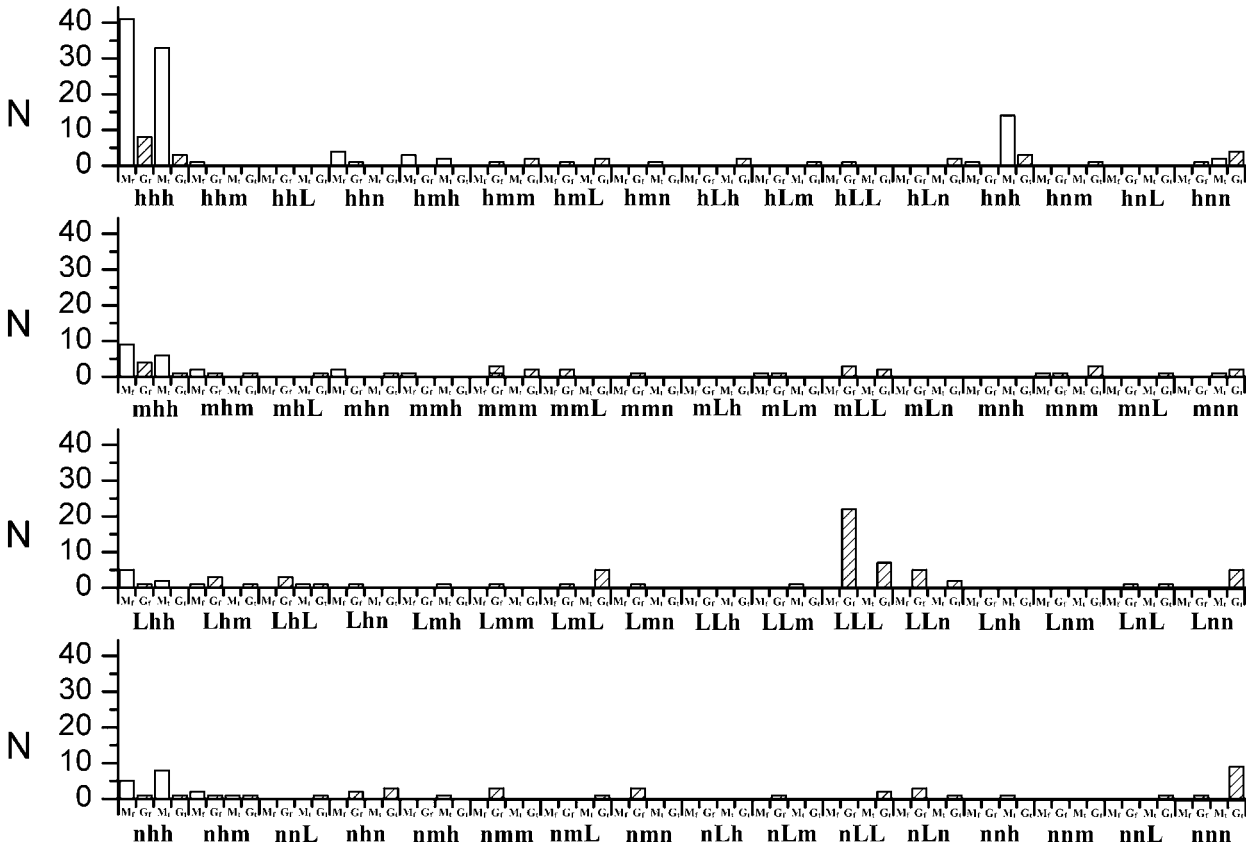

Figure 8. The distribution of frequency number N for 64 combination states of boundaries of 80 magnetic clouds. The front and tail M boundaries, M_f and M_t, are indicated by blank vertical bars, while the front and tail G boundaries, G_f and G_t, are indicated by shaded bars. The combinatory physical state is indicated under each set of boundaries, M_f, G_f, M_t, and G_t.

Table 2. Predominant Physical Combination States of the Cloud Boundaries

Physical states, T,D,β	Front Boundary Layer		Tail Boundary Layer	
	M_f Boundary	G_f Boundary	M_t Boundary	G_t Boundary
hhh	46(60%)	8(10%)	34(47%)	4(5%)
hh*	24(31%)	7(9%)	25(35%)	8(10%)
LLL	0(0%)	22(28%)	0(0%)	7(9%)
LL*	1(1%)	12(15%)	2(3%)	11(14%)
NNN	0(0%)	6(8%)	3(4%)	14(20%)
NN*	0(0%)	7(9%)	5(7%)	20(26%)

combinatory physical states are divided into four panels with each presenting 16 different combinatory states. The first letter of the combinatory states for each panel corresponds respectively to the temperature's four states: h, m, L, and n. The front and tail M boundaries are indicated by blank vertical bars labeled by M_f and M_t, respectively, while the front and tail G boundaries by shaded bars labeled by G_f and G_t, respectively. The various physical states are labeled under each set of boundary consisting of the four boundaries: M_f, G_f, M_t, and G_t. For example, the first state, "hhh," in the first panel means that T, N, and β all have relatively high readings for the M_f, G_f, M_t, and G_t boundaries, while the eleventh state, "LLL," in the third panel, implies that they all have low readings. The rest could be deduced similarly. The six predominant combinatory states in the frequency number distribution in Figure 8 are listed in Table 2. The asterisks in Table 2 mean that the physical state of a parameter are not specified. For example, "hh*" actually includes 12 combination states in which any two of the three parameters, T, N, and β, have relatively high readings to the adjacent background.

[19] Main results are summarized below:

[20] 1. Percentages of boundaries with "hhh" and "hh*" states are 91% for M_f boundary, 19% for G_f boundary, 82% for M_t boundary, and 15% for G_t boundary, respectively.

[21] 2. Percentages of boundaries with "LLL" and "LL*" states are 1% for M_f boundary, 41% for G_f boundary, 3% for M_t boundary, and 19% for G_t boundary, respectively.

[22] 3. Percentages of boundaries with "nnn" and "nn*" states are 0% for M_f boundary, 17% for G_f boundary, 11% for M_t boundary, and 46% for G_t boundary, respectively.

[23] 4. Other states of M and G boundary are randomly distributed, usually with low percentages of about 1–2%.

[24] From the results mentioned above, we can see that the absolutely predominant state in 64 combination states is "hhh" (or "hhh" + "hh") for the M boundary, either the front boundary M_f or the tail boundary M_t. Thus the M boundary may display some basic physical properties associated with a magnetic reconnection region, where the magnetic energy released by the magnetic field annihilation process contributes to heating the plasma and changing the plasma flow angle by adding a speed component parallel to the boundary layer. The enhanced plasma density may result from the extrusion on the magnetic reversed region from the cloud expansion, with a rise of plasma β as a natural result of the enhanced temperature and density and the reduced magnetic field, as shown in Figures 1–6.

[25] For the G boundary, the predominant physical state is "LLL" (or "LLL" + "LL*") with low temperature, low density, and low plasma β, displaying basic properties owned by a cloud body itself, which has not been intensively affected by the ambient flows. However, the two percentages 41% and 19% for G_f and G_t boundaries, respectively, are much lower than those for M_f and M_t boundaries (91% and 82%). Thus the physical states associated with G boundary given in the literature show a higher arbitrariness. In addition, the prominent percentages, 17% and 46%, of "nnn" and "nn*" states are also associated with G_f and G_t boundaries, respectively, which may be due to overemphasizing the magnetic signatures (a higher field intensity and a regular smooth rotated θ angle). The complexity in the interactions between the magnetic cloud body and the following flows, as shown in Figure 7, may also make it difficult to identify the G_t boundaries, as indicated by *Collier et al.* [2001].

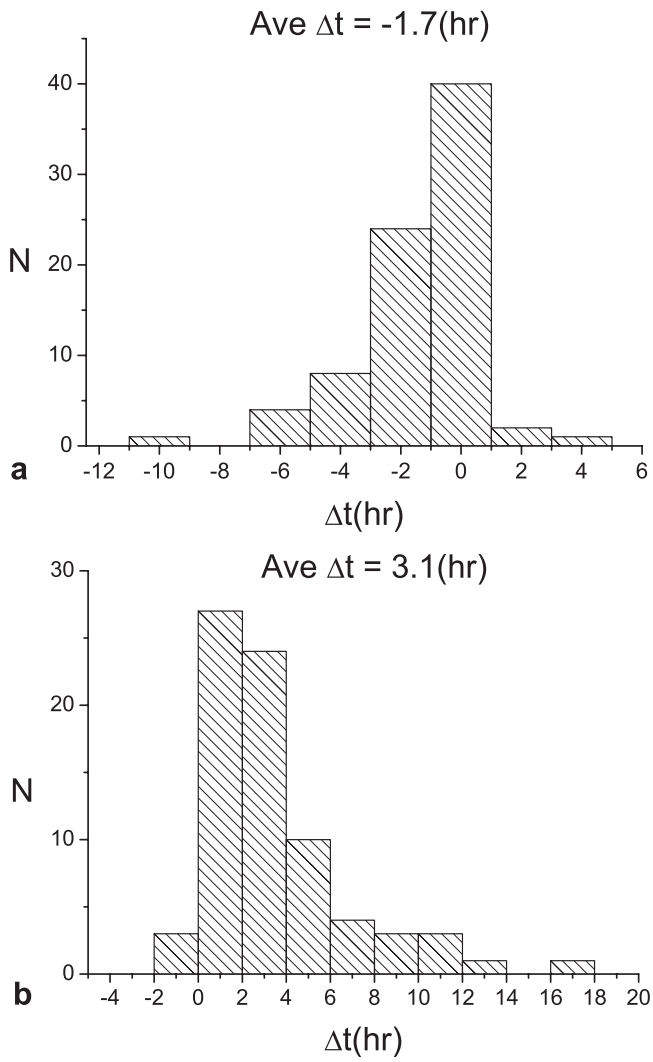

Figure 9. (a) The distribution of frequency number N for the time interval between M_f and G_f boundaries of 80 magnetic clouds. Average time interval, Δt, is calculated from the data listed in Table 1. (b) The distribution of frequency number N for the time interval between M_t and G_t boundaries of 80 magnetic clouds.

[26] Figures 9a and 9b show the distributions of time intervals between M_f and G_f boundaries and M_t and G_t boundaries, respectively, from the observed 80 magnetic clouds. It can be seen that more divergence is seen in the time interval between M_t and G_t boundaries. On average, the M_f boundary is earlier than the G_f boundary by about 1.7 hours, and the M_t boundary is later than the G_t boundary by about 3.1 hours, which are equivalent to typical spatial thickness of 2.5e6 and 4.5e6 km, respectively, for the front and boundary layer, if the speed of magnetic clouds is taken as 400 km/s. There are 15 cases that M_f and G_f boundaries are nearly coincident with each other and 12 cases that M_t and G_t boundaries are nearly coincident with each other. Actually, this coincidence only means that the time interval from the "hhh" state to the "LLL" state is so small that it could not be shown in low-resolution data. For example, it could be as small as 4–5 min, as shown in the 3 s average magnetic data on 18 October 1995 [*Lepping et al.*, 1997].

[27] Figures 10a–10h show the distributions of the changes in the azimuthal and latitude angles at M_f, M_t, G_f, and G_t boundaries, in bins of 20° and 10° (only for plotting convenience), respectively. Changes in the azimuthal angle, $\Delta\phi$, at M_f and M_t boundaries are centralized near 180°. Changes in the latitude angle, $\Delta\theta$, at M_f and M_t boundaries are more scattered than those of azimuthal angle, but peak values exists near 90°. At G_f and G_t boundaries, changes in the azimuth and latitude angles, $\Delta\phi$ and $\Delta\theta$, are randomly distributed compared with those at M_f and M_t boundaries, although at G_t boundaries they are centralized near $0 \sim 40°$ for both ϕ and θ angles. Notice that average changes in the azimuthal and latitude angles, calculated from the observed values at M boundaries listed in Table 1, about 180° and 90°, respectively, represent basic magnetic features of a magnetic reconnection region, but no clear physical meaning could be seen from the average changes in the azimuth and latitude angles, about 110° and 47°, at the G boundaries.

2.3. Identification of the Cloud Boundary Layers

[28] Based on the above-mentioned statistical analysis of 80 magnetic clouds, we propose that a magnetic cloud consists of the cloud body that preserves the basic properties of the magnetic cloud [*Burlaga*, 1991, 1995] and the boundary layer described below.

[29] The magnetic cloud boundary is a boundary layer that is formed through the interactions between the magnetic cloud and the interplanetary medium, rather than a simple discontinuity. Boundary layers ahead of clouds are called front boundary layers, while those following clouds are tail boundary layers. The boundary layer consists of the outer boundary (M_f), the interaction region, and the inner boundary (G_f). Outside the outer boundary of the layer is the interplanetary medium, while inside the inner boundary of the layer is the cloud body, which has not been strongly affected by the interaction and maintains basic properties of an expanding flux rope. Between the outer and the inner boundary of the layer is the region where the interaction has been mainly ongoing.

[30] The outer boundary is a possible magnetic reconnection boundary. It is usually identified by the field intensity drop (hole), the abrupt change of its azimuthal angle ($\sim$180°) and latitude angle ($\sim$90°), accompanied with the "hhh" or "hh*" state in the plasma temperature, density, and plasma β, which represents the basic plasma states of the magnetic reconnection region. The inner boundary, which separates the interaction region from the cloud body with an initial smooth rotation of the elevation angle and the enhanced field intensity, is usually associated with the "LLL" or "LL*" state, as a result of the expansion of the magnetic cloud. Between the outer and the inner boundary is the interaction reconnection region, where a physically meaningful interplay, a joint contribution of the magnetic reconnection process, and the expansion of the cloud, etc., determines the configuration of the boundary layer.

[31] The appeal of this scenario is its physical unambiguity and clarity and the manner it relates a large set of observations into a self-consistent whole. This identification can also help to overcome some inconsistencies in the determination of the cloud boundary. For example, why does the magnetic hole usually precede the drop in temperature? According to our definition, the former is the outer boundary of the boundary layer, while the latter is the inner boundary. Besides, considering the complexity and the turbulence of the interaction in the boundary layer and various spacecraft paths flying through them, asynchronous variation of the proton temperature, proton density, and associated plasma β parameter, etc., could be possible. Of course, this asynchronous variation brings us difficulty in identifying the M boundaries, especially in tail boundaries. Fortunately, such cases are limited.

3. Numerical Simulation Study

3.1. A Possible Formation Mechanism

[32] The formation mechanism of the magnetic cloud boundary is far from being answered, as could be seen from the inconsistency in identifying the cloud boundary. Based on the statistical study of boundaries of 80 magnetic clouds, a possible formation mechanism for the cloud boundary is suggested. Figure 11 displays the schematic physical picture of the formation mechanism of the cloud boundary. The cross section of the magnetic cloud, normal to the axis of the cloud, is indicated by a set of homocentric circles shown by dotted lines. The solid lines show the magnetic configurations in the background solar wind, the dashed lines denote the magnetic neutral lines, and the arrow indicates the motion direction of the magnetic cloud.

3.1.1. Front Boundary Layer

[33] The magnetic reconnection may take place in a small-scale interaction region where the front part of a magnetic cloud impacts on a magnetic reversal region. For example, this could be a local current sheet or the heliospheric current sheet, if the magnetic cloud moves at a speed higher than the solar wind speed as it propagates in interplanetary space. In this case the characteristic thickness of a local current sheet could be about $10^2 \sim 10^3$ km, far less than that of the large-scale background solar wind, 10^8 km. Since the magnetic diffusibility increases with the decreasing characteristic scale, the magnetic Reynolds number could decrease from $\sim 10^{10}$ to $\sim 10^{3-4}$ in interplanetary

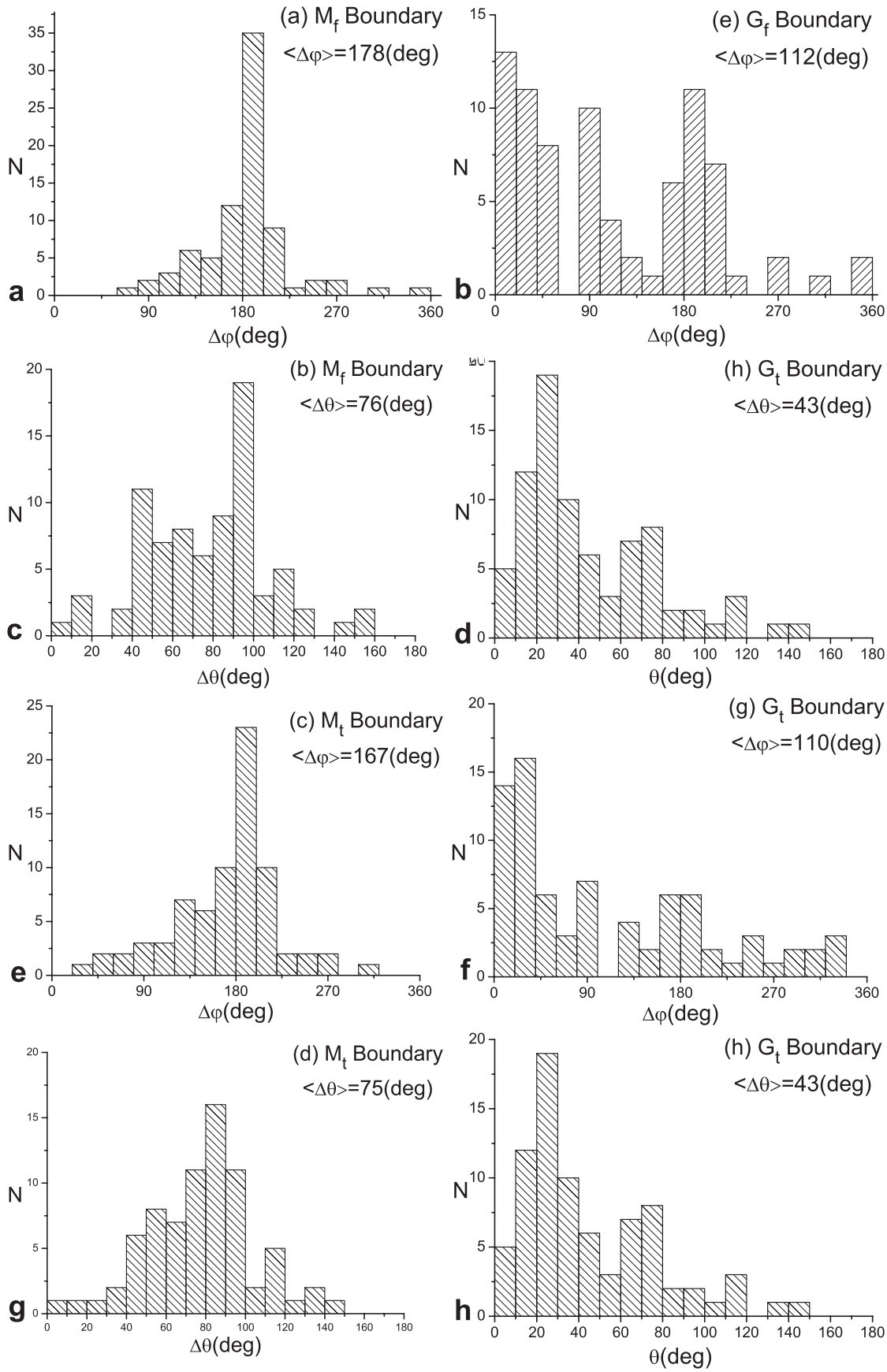

Figure 10. The distribution of frequency number N for the changes in the azimuthal and latitude angles ($\Delta\phi$ and $\Delta\theta$) at cloud boundaries of 80 magnetic clouds. (a–d) M boundary; (e–h) G boundary.

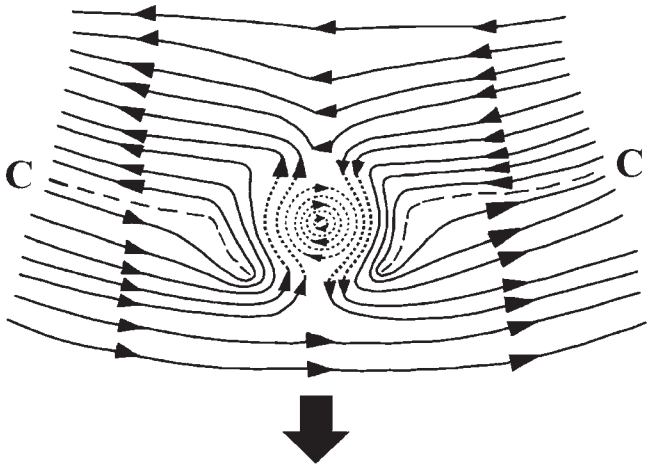

Figure 11. Schematic illustration of a magnetic cloud in the ambient medium, projected in the plane normal to the cloud axis. The large arrow indicates the motion direction of the magnetic cloud. The dashed lines show the magnetic neutral lines.

space. Consequently, the time scale for the diffusion of the magnetic field relative to the medium, L^2/η, is comparable to that for the removal of the field lines from the locality, L/V_A. Thus the frozen field theorem is locally invalid [*Axford*, 1984]. The magnetic reconnection process could possibly occur near this local current sheet of the small interaction region. The energy from the magnetic field annihilation contributes to the temperature enhancement in the boundary layer, and the pressure on the surrounding medium caused by the expansion of the magnetic cloud contributes to the density enhancement at the M boundary and in front of the main body of the cloud. Due to the decrease in the magnetic field strength and the enhancement in the proton temperature and density, plasma β is also high, resulting in the above-mentioned "hhh" or "hh*" state. Sometimes such evident characteristics may not be observed if the magnetic annihilation energy is not sufficient enough. Many other factors should be considered, such as the strong turbulent property of the interplanetary magnetic reconnection under a high magnetic Reynolds number ($>10^3$), the life span and the evolution of the magnetic reconnection region, the distance from the cloud source to the observation point, and the route along which the cloud passes through the spacecraft. However, the occurrence probability of the states "hhh" or "hh*" should be much higher than that of other states, as our statistical results indicates.

3.1.2. Tail Boundary Layer

[34] At the tail part of a magnetic cloud, as $V^2/2 + P/\rho$ is conserved along the streamlines following Bernoulli's principle, the flows overtaking the cloud and the flows around the cloud body transported tailward in the frame of reference related to the cloud will flow into the cloud at the speed higher than that of the cloud. This is due to the P/ρ reduction from the magnetic pressure depression and high background wind density compared with that in the cloud body. Thus the driving magnetic reconnection process could still possibly take place in the tail. On account of the kinematic complexity of the flows at the tail part of the cloud, the observed physical states of the tail M boundary present more turbulence than that of the front boundary, as indicated in the statistical result that the percentage of the "hhh" or "hh*" state at the tail boundary is much lower than that at its front counterpart. It is also expected that the magnetic configuration and the flow pattern at the tail boundary layer could be more complex than those at the front boundary layer. We notice in several cases the tail part of magnetic clouds could be overtaken by structures including corotating streams, another magnetic cloud, or perhaps followed by a prominence (i.e., filaments), etc., which makes the precise determination of the tail boundary nearly impossible.

3.1.3. Magnetic Neutral Line Region

[35] The heliospheric current sheet or local current sheet between the magnetic cloud and the ambient medium are indicated in Figure 11 by two dashed lines labeled with letter C. When the magnetic reconnection process occurs, the neutral line will surround two sides of the cloud body as the cloud moves relatively to it. In this case, the cloud could be embedded in a larger bidirectional electron event (BDE), with larger size than what has been documented. As *Crooker et al.* [1998] suggested, previously documented clouds identified by magnetic signatures are only parts of larger transient structures which occur more frequently at sector boundaries. So the magnetic cloud events are also frequently found near sector boundaries [e.g., *Klein and Burlaga*, 1982; *Bothmer and Rust*, 1997; *Crooker et al.*, 1998]. In the 80 magnetic clouds investigated here, about 35 clouds were observed near the heliospheric current sheet and neutral lines were frequently observed as cloud boundaries when a spacecraft traversed the heliospheric current sheets.

3.2. Preliminary Numerical Simulation

[36] A qualitative numerical simulation in physical principles has been performed to investigate the above-mentioned formation mechanism of the cloud boundary. It has been suggested that magnetic clouds have force-free flux-rope geometry [*Burlaga*, 1988, 1991, 1995; *Osheroivich and Burlaga*, 1997; *Marubashi*, 1997]. We adopt the plane normal to the cloud axis as our research plane, similar to the model presented by *Vandas et al.* [1993, 1995, 1997]. The magnetic field lines in a force-free configuration projected in this plane are a set of homocentric circles. While the cloud propagates in the background medium (including the corona and the interplanetary solar wind), since the azimuthal angle of helical magnetic field lines in the flux rope varies in the range of 360°, a local magnetic reversed region in favor of the magnetic reconnection process would form at either side of magnetic circles, regardless of the existence of current sheets in the background solar wind.

[37] A set of compressible two-dimensional MHD equations with three components (2.5 dimensions) is introduced as the governing equations, using a modified high-order TVD-Lax-Friedrichs scheme [*Feng et al.*, 2002]:

$$\frac{\partial U}{\partial t} + \frac{\partial F}{\partial x} + \frac{\partial G}{\partial y} = S,$$

where

$$U = \begin{bmatrix} \rho \\ \rho u \\ \rho v \\ \rho w \\ B_x \\ B_y \\ B_z \\ T \end{bmatrix}, \; F = \begin{bmatrix} \rho u \\ \rho u^2 + p - \dfrac{B_x^2 - B_y^2 - B_z^2}{2\mu_0} \\ \rho uv - \dfrac{B_x B_y}{\mu_0} \\ \rho uw - \dfrac{B_x B_z}{\mu_0} \\ 0 \\ uB_y - vB_x \\ uB_z - wB_x \\ Tu \end{bmatrix},$$

$$G = \begin{bmatrix} \rho v \\ \rho uv - \dfrac{B_x B_y}{\mu_0} \\ u^2 + p - \dfrac{B_x^2 - B_y^2 - B_z^2}{2\mu_0} \\ \rho vw - \dfrac{B_y B_z}{\mu_0} \\ -uB_y + vB_x \\ 0 \\ vB_z - wB_y \\ Tv \end{bmatrix}, \; S = \begin{bmatrix} \\ 0 \\ 0 \\ 0 \\ 0 \\ \dfrac{L(B_x)}{\sigma\mu_0} \\ \dfrac{L(B_y)}{\sigma\mu_0} \\ \dfrac{L(B_z)}{\sigma\mu_0} \\ \dfrac{T}{3}\left(\dfrac{\partial u}{\partial x} + \dfrac{\partial v}{\partial y}\right) \end{bmatrix}$$

and $L(\phi) = \frac{\partial^2 \phi}{\partial x^2} + \frac{\partial^2 \phi}{\partial y^2}$ is the Laplacian operator. We adopted the rectangular grid system. The number of grids perpendicular to the current sheet (Y direction) is two times larger than that parallel to the current sheet (X direction), and the step in X direction is two times longer than that in Y direction. The computation domain field is $X \times Y = 20 \times 20$. The initial background is the Harris symmetrical current sheet:

$$B_0(y) = B_\infty \tanh\left(\frac{y - y_0}{L}\right)\vec{e}_x.$$

[38] Assume that the cloud moves toward the current sheet from its initial position (x_0, y_0) = (0, 6), with certain initial speed. The magnetic Reynolds number Rm is 2000.

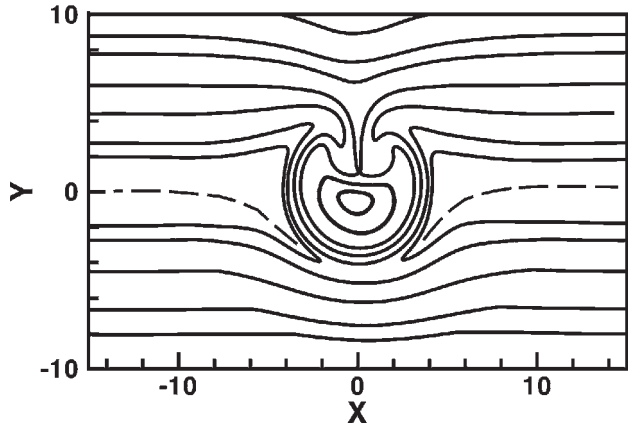

Figure 12. The pattern obtained from the numerical simulation under the typical interplanetary conditions. The cloud is moving in $-Y$ direction. The solid lines indicate the magnetic field lines, and the dashed lines show the neutral lines.

The cloud has the cylindrical force-free flux rope geometry with constant α given by *Lundquist* [1950]:

$$\begin{cases} B_r = 0 \\ B_\phi = B_\infty J_1(\alpha r) \\ B_z = B_\infty J_0(\alpha r), \end{cases}$$

where r is the radial distance from the axis, and J_0 and J_1 are Bessel functions. The result of the numerical simulation is shown in Figure 12 and Figure 13.

[39] Figure 12 shows the magnetic configuration when the magnetic reconnection process occurs in the front and tail part of a magnetic cloud. We can see that the magnetic reconnection region has formed in the front part of a cloud, as the cloud moves toward and pushes a current sheet at the speed of 0.5 V_A. Dashed lines in the figure indicate the neutral lines at both sides of the cloud. At the tail part of the cloud, the driving magnetic reconnection process also takes place as the flows overtake the cloud, following the Bernoulli principle. However, the magnetic configurations at the tail part of the cloud are distinctly different from those in the front part, due to its complex flow pattern compared with that at the front part of the cloud. It is clear that the preliminary physical picture from the numerical simulation is consistent with the qualitative physical scenario plotted in Figure 11 based on the statistical analysis in section 2, except for the details of the tail flow pattern. We may expect that the magnetic neutral lines at the two sides of the cloud body would be more and more bended, therefore being frequently observed as the cloud motions forward (in Figure 11, downward), when a spacecraft traverses the cloud from various directions.

[40] Figure 13 shows the profile of the physical parameters recorded along the path in the X = 0 direction in Figure 12, where obvious features of the boundary layer could be easily seen. At either side of the cloud, the M_f and M_t boundaries determined via the MRB criterion, marked by solid lines, indicate an abrupt decrease in the magnetic field strength, an abrupt change of about 180° in the azimuthal

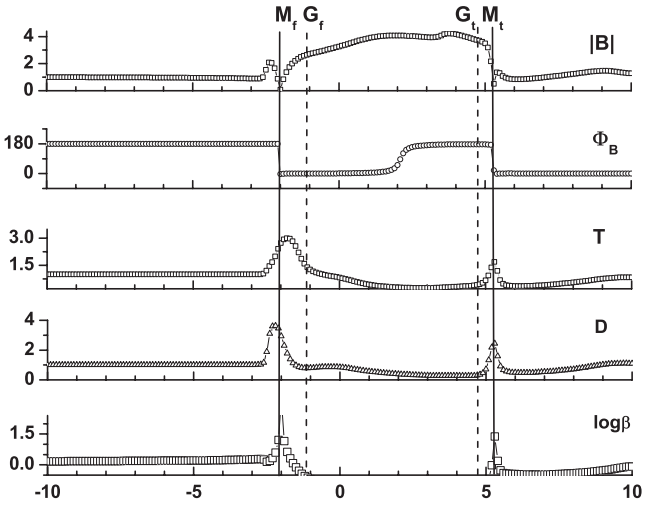

Figure 13. Physical parameters recorded along the path that X equals zero in Figure 12. The panels show from top to bottom the magnetic field magnitude $|B|$, the azimuthal angle Φ, the temperature T, density N, and the logarithm of plasma β.

angle, and the corresponding high readings of temperature T, density N, and β, i.e., "hhh" state, due to the occurrence of the magnetic reconnection process. The G_f and G_t boundaries, marked by dashed lines, are located in the inner side of the M boundary and associated with relatively high magnetic field strength and low temperature, density, and plasma β, determined via the usual method. These preliminary simulation results may qualitatively explain some observed basic characteristics of the magnetic cloud boundaries shown in the statistical analysis and in Figures 1–7. They should clarify some inconsistencies in previously identified cloud boundaries. In addition, it can be seen from Figure 13 that the sizes of magnetic clouds, defined by the magnetic reconnection boundaries, M_f and M_t, are larger than those bounded by the documented G_f and G_t boundaries. This is consistent with the conclusion obtained by *Crooker et al.* [1998] in studying the magnetic clouds near the heliospheric current sheets.

4. Fine Structures Inside the Magnetic Cloud Boundary Layer

[41] The magnetic cloud boundary is not a simple boundary but a complex boundary layer, whose outer and inner boundaries are mostly discontinuities. If our idea for the magnetic cloud boundary layer is primarily correct, the behavior of the magnetic field and the solar wind plasma would be altered across the boundary layer. That is to say, the boundary layer should own certain structures different from those ahead of and behind it. What are the fine structures inside the cloud boundary layer? As an example, the variations of the southward component of the magnetic field across the boundary layer may shed some light on such a question. Figure 14 shows the probability distribution function of the interplanetary southward component across the boundary layer of the magnetic cloud on 2 August 1995 observed by the WIND spacecraft. The intervals of the data sampling are: 0210–0250 UT for the background medium before the M boundary, 0250–0330 UT for the boundary layer and 0330–0410 UT for the cloud after the G boundary. The resolution of the magnetic field data is 3 s. The panels in Figure 14 show from top to bottom that the average interplanetary $\overline{B_z}$ rotates southward across the M boundary from $\overline{B_z}$ = 0.25 nT before the M boundary to $\overline{B_z}$ = −8.4 nT inside the boundary layer, and $\overline{B_z}$ = −10.8 nT after the G boundary into the cloud. Besides the enhancement in the southward component, the probability distribution function also undergoes significant changes across the boundary layer. The distribution function inside the boundary layer implies strong turbulence compared with that in the ambient medium and in the cloud, and the fluctuations after the G boundary are extremely low, almost unaffected by the interactions in the boundary layer. It is interesting to ask whether the prominent changes in the probability distribution function of the southward component across the boundary layer will affect the efficiency of the magnetic reconnection in the cloud-magnetosphere coupling, therefore affecting the transferring of energy, momentum, and mass from the solar wind into the magnetosphere. In a sense it might be closer to physical reality to discuss the cloud-magnetosphere coupling based on the investigation of the interaction between the boundary layer and the magnetosphere. As *Tsurutani and Gonzalez* [1997] indicated in a review of the interplanetary causes of magnetic storms, because of the importance of the sheath fields, the intensity and duration of geomagnetic storms cannot be predicated by solar observations of active regions alone. Therefore for most of magnetic clouds without the "sheath" we specu-

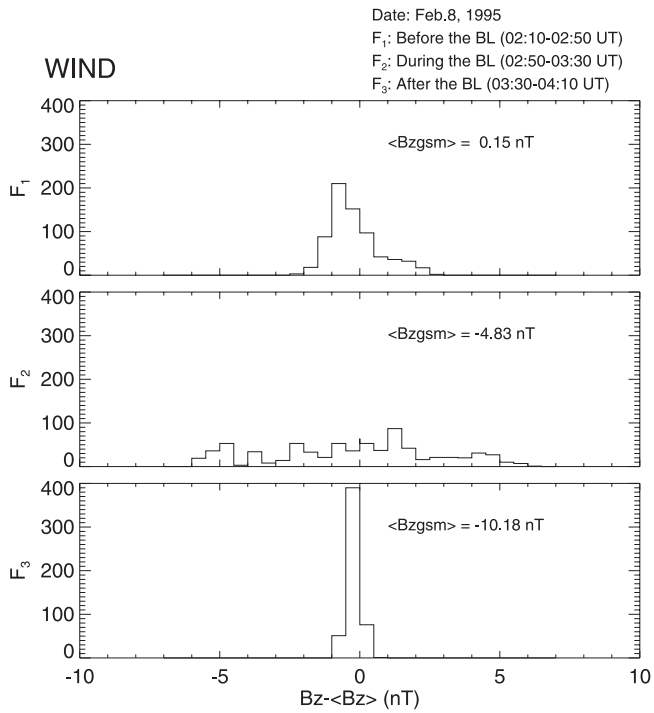

Figure 14. The fluctuation distributions of southward component B_z across the boundary layer of the magnetic cloud on 2 February 1995. Three-second magnetic field data of Wind spacecraft are adopted.

lated that the role of the boundary layer structures would be important in the geomagnetic effects. Because the Earth is immersed in the boundary layer with a typical thickness of about 200 $\sim$ 350 radius of the Earth in terms of its temporal scale of 1.7 $\sim$ 3.1 hours, the fine structures inside the layer could affect the geomagnetic storm processes. Anyway, the properties and structures of the boundary layer, which are distinctly different from the background solar wind and the cloud, further rationalize the boundary layer concept.

5. Discussions and Conclusions

[42] We have noted that magnetic-hole-like structures just ahead of magnetic clouds have been occasionally reported by some authors and were suggested to be associated with the magnetic reconnection process [*Burlaga*, 1995; *Farrugia et al.*, 2001]. *Farrugia et al.* [2001] identified a rotational discontinuity and a slow shock before the magnetic hole ahead of the magnetic cloud on 24 December 1996 and interpreted the whole structure as a reconnection layer according to the Petschek-type reconnection theory. Recently, *Zurbuchen et al.* [2001] concluded that microscale magnetic holes very likely develop in the heliosphere and are not of direct solar origin. Now our question is: If magnetic reconnection may occur between magnetic clouds and the ambient medium, what is the spatial scope for the magnetic reconnection process to take place? How does the reconnection region evolve in interplanetary space? When a prominence erupts, the flowing prominence material is often observed spiraling and outlining helical structures, suggesting that ropes of helical magnetic field embeds the erupted prominence [*Tandberg-Hanssen*, 1995]. In the static model of solar corona proposed by *Low and Hundhausen* [1995], a force-free flux rope, which would expand and rise into interplanetary space during a CME eruption, threads through an arcade of closed field lines under a coronal steamer. A close relationship between magnetic field configurations of magnetic clouds and solar magnetic fields around the solar filaments has also been reported [*Marubashi*, 1986, 1997; *Bothmer and Schwenn*, 1994; *Rust*, 1994; *Bothmer and Rust*, 1997]. The possibility that a magnetic cloud may be the interplanetary counterpart of the helmet streamer flux-rope is substantiated by a case of a magnetic cloud containing prominence material in January 1997, reported by *Burlaga et al.* [1998]. We have known that the magnetic field lines in the flux rope are assumed to be a family of helices and the pitch angle of the field lines increases with increasing distance from the axis, reaching the asymptotic form of circles on the outer part. Hence even if the cloud is embedded in the interplanetary magnetic field with uniform polarity without the heliospheric current sheet, the magnetic reversed region would surely form on one side of the rope in interplanetary space, resulting in the formation of the local current sheet. Actually, magnetic clouds extend up to about 60° in the longitudinal direction in interplanetary space, comparable to one astronomical unit at 1 AU, and their radial size is in the range of 0.2–0.4 AU. With such large spatial scales, magnetic clouds with their origins in the latitudinal range of ±45° on the solar surface would very likely encounter the heliospheric current sheet as they propagate in interplanetary space. About half of magnetic clouds could be associated with sector boundaries, because CMEs, the source of magnetic clouds, mostly occur in the coronal streamer belt, as *Crooker et al.* [1998] indicated. However, in the magnetic configuration suggested by Low and Hundhausen, magnetic reversed regions would not be so easily formed, except when the flux rope rises and expands, leading to collapse of the coronal streamer system. As a result of the sustaining impact on the local current sheet or the heliospheric current sheet, due to the expansion of the cloud, the magnetic reconnection process may occur near the magnetic reversed region in the corona or interplanetary space where the frozen field theorem could be locally invalid, depending on the local conditions and the cloud structure. Both our observational analysis and numerical simulations have shown that the magnetic reconnection process does occur under typical interplanetary conditions with a Reynolds number Rm = 2000 $\sim$ 10000 [*Wei et al.*, 1997, 2000, 2001]. An evidence of interplanetary magnetic reconnection of a noncoronal mass ejection flux rope was reported by *Moldwin et al.* [1995].

[43] Furthermore, how long will the signatures of the magnetic reconnection boundary persist? It is an important problem related to the evolution of the magnetic cloud. After the magnetic reconnection process occurs reconnection conditions would be weakened and the frozen-in condition would be gradually recovered. The historical information of the magnetic reconnection process is also partly "frozen" in the cloud. However, the cloud may be still "potential" for further magnetic reconnection. This process may continue to repeat itself until the cloud is unable to drive further magnetic reconnection with a gradual depression in its dynamic pressure and relative speed to the background waned. Therefore various widths of the boundary layer and structures of the cloud body would be observed. Due to the turbulence under a high Reynolds number, signatures of the boundary layer would frequently be observed but not be very prominent. It is still hard to know the time interval between the two magnetic reconnection processes at present. Much more work needs to be done to answer these questions.

[44] When the magnetic reconnection process occurs, the magnetic flux in the flux rope would decrease, as if magnetic fields "peel off" from the magnetic cloud. If such a peeling-off process goes quickly enough, the spatial scale of the cloud would diminish gradually. The magnetic cloud given in Figure 6, with its temporal scale of $\sim$4–5 hours, may be such a case. Further study for this problem is necessary.

[45] We also note that although noticeable features of magnetic reconnection regions are usually observed at front boundaries, it is sometimes not the case at tail boundaries. In several cases the tail parts of magnetic clouds appear to merge into the ambient solar wind and it is then almost impossible to clearly identify the cloud boundary. This may be due to the cloud being overtaken by corotating streams, shock waves, prominence, or even another cloud. These flows contribute to the driving magnetic reconnection process at the tail part of a cloud but also appear to break up and "erase" this magnetic reconnection region. Approximately a third of the magnetic clouds are overtaken by fast flows [*Klein and Burlaga*, 1982], and shocks or shock-like structures are also reported inside the tail part of the cloud

body [e.g., see *Lepping et al.*, 1997; *Collier et al.*, 2001]. In these cases, the interactions would be very complicated. In the 80 magnetic clouds investigated here, about 20 clouds follow by the fast flow. Another interesting question is that the size of magnetic clouds defined by the magnetic reconnection boundaries (M_f and M_t) with the "hhh" state are almost larger than the documented G_f and G_t boundaries with the "LLL" state. Sometimes, the former not only contains the latter with a monotonic change in θ from a angle θ_0 at the beginning time of clouds to the maximum value θ_m at the ending time but also a continual smooth rotation almost to the original θ_0. Similarly, the ϕ angle also tends to rotate continually to the original ϕ_0 at the beginning of the magnetic cloud. Generally, the plasma parameters in clouds, such as proton temperature, density, velocity, and plasma β, still continue to remain the cloud's proper values, as shown in Figures 2, 5, and 6. Of 80 samples, about 30 magnetic clouds have a "sine" profile in θ. For this point a possible schematic illustration has been proposed by *Crooker et al.* [1998]. Besides, the interplanetary manifestations of CMEs is still an interesting problem. The front boundary layers of about 20 clouds could be speculated as the outer loops of CMEs based on the observed characteristics reported by *Galvin et al.* [1987] and *Tsurutani et al.* [1998]. However, the tail boundary layers of the clouds investigated here could hardly be identified as being associated with the filaments of CMEs, except for the event in January 1997 [*Burlaga et al.*, 1998].

[46] In conclusion, the magnetic cloud boundaries are complex boundary layers with their own structures, rather than simple boundaries. Most front boundary layers could possibly form through the magnetic reconnection process as a result of the interactions between magnetic clouds and the convected loops when the magnetic clouds propagate through the corona or in interplanetary space after they are ejected from the Sun. However, the filaments of CMEs could not be associated with the tail boundary layers of the 80 clouds investigated here. Most outer boundaries of the boundary layers could be magnetic reconnection boundaries associated with the "hhh" or "hh*" state, while the inner boundaries, which separate the boundary layers from the expanding cloud bodies, are mostly associated with "LLL" or "LL*" states. This physical formation mechanism of the cloud boundary layer, supported by the preliminary numerical simulations, could qualitatively explain some spacecraft observations of magnetic clouds and could also help overcome some inconsistencies in identifying cloud boundaries and relate some seemingly paradoxical phenomena into a self-consistent whole. The average time scales of the boundary layers are 1.7 hours and 3.1 hours for the front and tail boundary layer, respectively. The boundary layer owns special fine structures different from the ambient solar wind and the cloud body itself, which also support the boundary layer concept suggested in this paper. The remarkable changes of the probability distribution function of the southward field component across the boundary layer may have important effects on cloud-magnetosphere coupling, therefore affecting geomagnetic activity and other space weather processes. Other physical states, structures, and the evolution of the boundary layer still need to be studied further.

[47] **Acknowledgments.** We would like to express our thanks to the reviewers for their valuable suggestions on the basis of which the paper has been improved. We appreciate NASA CDAWEB for publishing the WIND and IMP8 magnetic field and solar wind data. We are greatly indebted to R. Schwenn for permitting us to use Helios data. We are also grateful to the Wind MFI (PI, R. Lepping, GSFC) team for identifying the magnetic clouds observed by the WIND spacecraft. We acknowledge the beneficial conversations with J. K. Chao. This work was jointly supported by the National Key Basic Research Science Foundation of China (grant G200078405) and the National Natural Science Foundation of China (grants 40274052, 49990450, and 49874040).

[48] Lou-Chuang Lee thanks Bruce Tsurutani and another reviewer for their assistance in evaluating this paper.

References

Axford, W. I., Magnetic field reconnection, in *Magnetic Reconnection in Space and Laboratory Plasmas*, *Geophys. Monogr. Ser.*, vol. 30, edited by E. W. Hones Jr., p. 1, AGU, Washington, D.C., 1984.

Bothmer, V., The structure of magnetic clouds in solar wind, *MPAE-W-100-93-10*, pp. 151–161, Max Plank Inst. für Aeron., Katlenburg-Lindau, Germany, 1993.

Bothmer, V., and D. M. Rust, The field configuration of magnetic clouds and the solar cycle, in *Coronal Mass Ejections*, *Geophys. Monogr. Ser.*, vol. 99, edited by N. Crooker et al., pp. 139–146, AGU, Washington, D.C., 1997.

Bothmer, V., and R. Schwenn, Eruptive prominences as sources of magnetic clouds in the solar wind, *Space Sci. Rev.*, *70*, 215–220, 1994.

Burlaga, L. F., Magnetic clouds: Constant alpha force-free configurations, *J. Geophys. Res.*, *93*, 7217–7224, 1988.

Burlaga, L. F., Magnetic clouds, in *Physics of the Inner Heliosphere*, vol. 2, edited by R. Schwenn and E. March, pp. 1–22, Springer-Verlag, New York, 1991.

Burlaga, L. F., *Interplanetary Magnetohydrodynamics*, Oxford Univ. Press, New York, 1995.

Burlaga, L. F., et al., Interplanetary particles and fields, November 22 to December 6, 1977: Helios, Voyager and IMP Observations between 0.6 AU and 1.6 AU, *J. Geophys. Res.*, *85*, 2227–2242, 1980.

Burlaga, L. F., S. F. Mariani, and R. Schwenn, Magnetic loop behind an interplanetary shock: Voyager, Helios and IMP8 observations, *J. Geophys. Res.*, *86*, 6673–6684, 1981.

Burlaga, L. F., et al., A magnetic cloud containing prominence material: January 1997, *J. Geophys. Res.*, *103*, 277–285, 1998.

Chao, J. K., C. B. Wang, D. J. Wu, and R. P. Lepping, Interaction of the Oct. 14–19, 1995 magnetic cloud with a solar interplanetary disturbance, *Eos Trans, AGU*, *80*(17), Spring Meet. Suppl., S269, 1999.

Chapman, S., and V. C. A. Ferraro, Solar streams of corpuscles, their geometry, absorption of light and penetration, *Mon. Not. R. Astron. Soc.*, *89*, 470, 1929.

Cocconi, G., T. Gold, K. Greisen, S. Hayakawa, and J. P. Morrison, The cosmic ray flare effect, *Nuovo Cimento*, *8*, 161, 1958.

Collier, M. R., et al., Reconnection remnants in the magnetic cloud of October 18–19 1995: A shock, monochromatic wave, heat flux dropout, and energetic ion beam, *J. Geophys. Res.*, *106*, 15,985–16,000, 2001.

Crooker, N. U., J. T. Gosling, and S. W. Kahler, Magnetic clouds at sector boundaries, *J. Geophys. Res.*, *103*, 301–306, 1998.

Fainberg, J., et al., Observations of electron and proton components in a magnetic cloud and related wave activity, in *Solar Wind Eight*, edited by D. Winterhalter et al., *AIP Conf. Proc.*, *382*, 554–560, 1995.

Farrugia, C. J., et al., Observations in the sheath region ahead of magnetic clouds and in the dayside magnetosheath during cloud passage, *Adv. Space Res.*, *14*, 105–109, 1994.

Farrugia, C. J., R. P. Lepping, L. F. Burlaga, A. Szabo, D. Vassiliadis, P. Stauning, and M. P. Freeman, The Wind magnetic cloud of October 18–20, 1995: Implications for the magnetosphere, *Eos Trans. AGU*, *77*(17), Spring Meet. Suppl., S241, 1996.

Farrugia, C. J., L. F. Burlaga, and L. P. Lepping, Magnetic clouds and the quiet-storm effect at earth, in *Magnetic Storms*, edited by B. T. Tsurutani et al., pp. 91–106, AGU, Washington, D.C., 1997.

Farrugia, C. J., P. E. Sandhalt, J. Moen, and R. L. Arnoldy, Unusual features of the January 1997 magnetic cloud and their effect on optical dayside auroral signatures, *Geophys. Res. Lett.*, *25*, 3051–3054, 1998.

Farrugia, C. J., et al., A reconnection layer associated with a magnetic cloud, *Adv. Space Res.*, *28*, 759–764, 2001.

Feng, X., S. T. Wu, Q. Fan, and F. Wei, A class of TVD type combined numerical scheme for MHD equations and its application to MHD numerical simulations, *Chinese J. Space Sci.*, *22*, 316–323, 2002.

Galvin, A. B., F. M. Ipavich, G. Gloeckler, D. Hovestadt, S. J. Bame, B. Klecker, M. Scholer, and B. T. Tsurutani, Solar wind iron charge states preceeding a driver plasma, *J. Geophys. Res.*, *92*, 12,069, 1987.

Gold, T., Magnetic storms, *Space Sci. Rev.*, *1*, 100, 1962.
Gonzalez, W. D., and B. T. Tsurutani, Criteria of interplanetary parameters causing intense magnetic storms(Dst < −100 nT), *Planet. Space Sci.*, *35*, 1101–1109, 1987.
Gosling, J. T., Coronal mass ejections: An overview, in *Coronal Mass Ejections*, *Geophys. Monogr. Ser.*, vol. 99, edited by N. Crooker et al., pp. 9–16, AGU, Washington, D.C., 1997.
Gosling, J. T., D. N. Baker, S. J. Bame, W. C. Feldman, and R. Zwickl, Bidirectional solar wind electron heat flux events, *J. Geophys. Res.*, *92*, 8519–8535, 1987.
Janoo, L., Feld and flow perturbation in the October 18–19 1995, magnetic cloud, *J. Geophys. Res.*, *103*, 17,249–17,259, 1998.
Klein, L. W., and L. F. Burlaga, Interplanetary magnetic clouds at 1 AU, *J. Geophys. Res.*, *87*, 613–624, 1982.
Larson, D. E., et al., Tracing the Topology of the October 18–20, 1995, Magnetic cloud with ∼0.1–102 Kev electrons, *Geophys. Res. Lett.*, *24*, 911–914, 1997.
Lepping, R. P., J. A. Jones, and L. F. Burlaga, Magnetic field structure of interplanetary magnetic clouds at 1 AU, *J. Geophys. Res.*, *95*, 11,957–11,965, 1990.
Lepping, R. P., et al., The WIND magnetic cloud and events of October 18–20, 1995: Interplanetary properties and as triggers for geomagnetic activity, *J. Geophys. Res.*, *102*, 14,049–14,063, 1997.
Lepping, R. P., D. Berdichersky, A. Szabo, A. J. Lazarus, and B. J. Thompson, Upstream shocks and interplanetary magnetic cloud speed and expansion: Sun, wind, and Earth observations, *Adv. Space Res.*, *26*, in press, 2001.
Low, B. C., and J. R. Hundhausen, Magnetostatic structures of the solar corona II: The magnetic topology of quiescent prominences, *Astrophys. J.*, *443*, 818, 1995.
Lundquist, S., Magnetohydrostatic fields, *Ark. Fys*, *2*, 361, 1950.
Marsden, R. G., T. R. Sanderson, C. Tranquiller, and K.-P. Wenzel, ISEE-3 observations of low energy proton bidirectional events and their relation to isolated interplanetary magnetic structures, *J. Geophys. Res.*, *92*, 11,009–11,019, 1987.
Marubashi, K., Structures of the interplanetary magnetic clouds and their regions, *Adv. Space Res.*, *6*, 335–338, 1986.
Marubashi, K., Interplanetary magnetic flux ropes and solar filaments, *Coronal Mass Ejections*, *Geophys. Monogr. Ser.*, vol. 99, edited by N. Crooker et al., pp. 147–156, AGU, Washington, D.C., 1997.
Moldwin, M. B., et al., Ulysses observation of a noncoronal mass ejection flux rope: Evidence of interplanetary magnetic reconnection, *J. Geophys. Res.*, *100*, 19,903–19,910, 1995.
Morrison, P., Solar-connection variations of the cosmic rays, *Phys. Rev.*, *95*, 616, 1954.
Osherovich, V., and L. F. Burlaga, Magnetic clouds, *Coronal Mass Ejections*, *Geophys. Monogr. Ser.*, vol. 99, edited by N. Crooker et al., pp. 157–168, AGU, Washington, D.C., 1997.
Osherovich, V. A., et al., Polytropic relationship for magnetic clouds, *J. Geophys. Res.*, *98*, 15,331–15,342, 1993.
Rust, D. M., Spawning and shedding helical magnetic fields in the solar atmosphere, *Geophys. Res. Lett.*, *21*, 241–244, 1994.
Tandberg-Hanssen, E., *Solar Prominences*, Kluwer Acad., Norwell, Mass., 1995.
Tsurutani, B. T., and W. D. Gonzalez, The interplanetary causes of magnetic storms: A review, in *Magnetic Storms*, *Geophys. Monogr. Ser.*, vol. 98, edited by B. T. Tsurutani et al., pp. 77–89, AGU, Washington, D.C., 1997.
Tsurutani, B. T., W. D. Gonzalez, F. Tang, S. I. Akasofu, and E. J. Smith, Origin of interplanetary southward magnetic fields responsible for major magnetic storms near solar maximum (1978–1979), *J. Geophys. Res.*, *93*, 8519, 1988.
Tsurutani, B. T., W. D. Gonzalez, F. Tang, and Y. T. Lee, Great magnetic storms, *Geophys. Res. Lett.*, *19*, 73–76, 1992.
Tsurutani, B. T., et al., The January 10, 1997 auroral hot spot, horseshoe aurora and first substorm: A CME loop?, *Geophys. Res. Lett.*, *25*, 3047–3050, 1998.
Vandas, M., S. Fischer, P. Pelant, and A. Geranios, Evidence for a spheroidal structure of magnetic clouds, *J. Geophys. Res.*, *98*, 21,061–21,069, 1993.
Vandas, M., et al., Simulation of magnetic cloud propagation in the inner heliosphere in two dimensions: 1. A loop perpendicular to the ecliptic plane, *J. Geophys Res.*, *100*, 12,285–12,292, 1995.
Vandas, M., S. Fischer, D. Odstrail, M. Dryer, Z. Smith, and T. Detman, Flux ropes and spheromaks, A numerical study, in *Coronal Mass Ejections*, *Geophys. Monogr. Ser.*, vol. 99, edited by N. Crooker et al., pp. 169–176, AGU, Washington, D.C., 1997.
Wei, F., R. Schwenn, and Q. Hu, Magnetic reconnection events in the interplanetary space, *Sci. China, Ser. E*, *40*, 463–471, 1997.
Wei, F., Q. Hu, R. Schwenn, and X. Feng, Simulation of turbulent magnetic reconnection in the small scale solar wind, *40: Sci. China, Ser. A*, *43*, 629–637, 2000.
Wei, F., Q. Hu, and X. Feng, Numerical study of magnetic reconnection process near interplanetary current sheet, *Chinese Sci. Bull.*, *46*, 111–116, 2001.
Wilson, R. M., On the behavior of the Dst Geomagnetic Index in the vicinity of magnetic clouds passages at Earth, *J. Geophys. Res.*, *95*, 215–219, 1990.
Zhang, G., and L. F. Burlaga, Magnetic clouds, geomagnetic disturbances, and cosmic ray decreases, *J. Geophys. Res.*, *93*, 2511–2518, 1988.
Zurbuchen, F. H., S. Hefti, L. A. Fisk, G. Gloeckler, N. A. Schwadrom, C. W. Smith, N. F. Ness, R. M. Skoug, D. J. McComas, and L. F. Burlaga, On the origin of microscale magnetic holes in the solar wind, *J. Geophys. Res.*, *106*, 16,001–16,010, 2001.

Q. Fan, X. Feng, R. Liu, and F. Wei, SIGMA Weather Group, Key Laboratory for Space Weather, Center for Space Science and Applied Research, Chinese Academy of Sciences, P. O. Box 8701, Beijing, 100080, China. (glfan@spaceweather.ac.cn; fengx@spaceweather.ac.cn; rliu@spaceweather.ac.cn; fswei@spaceweather.ac.cn)